FACULTY OF PHARMACEUTICAL SCIENCES

Optimizing a QuEChERS-based UHPLC-MS/MS approach used for the analysis of multiple aflatoxins in Italian-produced peanuts.

Valérie Coussens

A Master dissertation for the study programme Master in Pharmaceutical Care

Academic year: 2022 – 2023

GHENT UNIVERSITY

ABSTRACT

Mycotoxins are secondary metabolites from fungi. Aflatoxins (AFTs) are mycotoxins produced by the fungi *A.flavus, A. parasiticus,* and others. There are multiple kinds of AFTs, the main ones being AFB1, AFB2, AFG1, and AFG2. They can contaminate food and feed such as grains, spices, cereals, nuts, etc. AFTs are a serious threat to the health of humans and animals. Many dangerous properties have been observed and contributed to them such as teratogenic, hepatotoxic, carcinogenic, and nephrotoxic effects. Peanuts are easily contaminated as they grow in warm and moist climates in soil. Ideal conditions for the colonisation of these nuts with AFT-producing fungi. Peanuts are a main protein source and can be found in many people's diets. This thesis focuses on the contamination of peanuts with aflatoxins B1, B2, G1, and G2.

HPLC-MS/MS is currently the most used method for detecting and analysing AFT contamination in food. Before this sample preparation is needed. This is to eliminate matrix components that can interfere with the response of the AFTs. These purifying steps are differently optimised for each food matrix, as they have other consistencies. The goal of this thesis is to find a more efficient and faster but trustworthy clean-up approach for peanut samples. Peanuts are a complex matrix and optimization of current existing methods is necessary to save time and resources.

Before starting practical work, multiple studies were compared through literature study. The focus is on the sample preparation and extraction steps. The two most promising studies were chosen. Both approaches were then performed experimentally on blank peanut samples that are spiked with a standard AFT solution. The samples were prepared according to these two protocols, then analysed using triple quadrupole UHPLC-MS/MS. The choice for the best one was made and performed on the samples of interest, the peanuts grown in Italy. These were first screened for mycotoxins using IM-MS-TOF. No AFTs were found in the peanuts. A validation method was realized in the triple QQQ, and future studies can be done regarding the mycotoxin contamination of peanuts.

SAMENVATTING

Mycotoxines zijn secundaire metabolieten van fungi. Aflatoxines (AFTs) zijn mycotoxines worden geproduceerd door bv. *A. flavus* en *A. parasiticus.* Er zijn meerdere soorten AFTs, de belangrijkste zijn aflatoxine B1, B2, G1 en G2. Ze kunnen voedsel zoals granen, noten, kruiden,… contamineren. AFTs zijn een ernstige bedreiging voor de gezondheid van mens en dier. Veel nefaste eigenschappen zijn aan hen toegeschreven, bijvoorbeeld carcinogene, teratogene, hepatotoxische en nefrotoxische effecten. Pinda's worden gemakkelijk gecontamineerd doordat ze in grond worden gekweekt in warme en vochtige klimaten. Dit zijn ideale condities voor kolonisatie van pinda's met AFT-producerende fungi. Pinda's zijn een belangrijke eiwit bron en komt voor in het dieet van velen. Onze focus ligt op de contaminatie van pinda's met AFB1, AFB2, AFG1 en AFG2.

HPLC-MS/MS is momenteel de meest gebruikte methode om AFT contaminatie op te sporen en te analyseren in voedsel. Voor de analyse is sample preparation nodig. Dit is om matrix elementen die interfereren met de respons van de AFTs te elimineren. Deze opzuivering is anders voor elke matrix omdat zij elk een andere samenstelling hebben. Het doel in deze thesis is om efficiëntere en snellere, maar betrouwbare clean-up methode te vinden voor pinda's. Pinda's zijn een complexe matrix en de optimalisatie van de bestaande methoden is nodig om tijd en materialen te besparen.

Voor de start van het praktische werk werden verschillende onderzoeken vergeleken via literatuurstudie. De nadruk lag vooral op de sample preparation en extractie stappen. Twee veelbelovende studies werden uitgekozen. Deze twee methoden werden dan experimenteel uitgevoerd op blanco pindastalen dat gespiked werden met een standaard AFT mengsel. Deze stalen werden nadien geanalyseerd met behulp van triple quadrupole (QQQ) UHPLC-MS/MS. Er werd gekozen voor de methode met de beste resultaten. Nadien werd deze methode uitgevoerd op de stalen van onze interesse, de pinda's uit Italië. Deze werden eerst gescreend op mycotoxinen met IM-MS-TOF. Er werden geen AFTs gevonden in de pinda's. Wel werd een validatie methode gerealiseerd in de triple QQQ om in de toekomst mycotoxinen in pinda's te analyseren.

ACKNOWLEDGEMENTS

I would like to thank everyone who helped bring this work to a good end. This work would not have been achieved without the help and guidance of many people.

First, I want to express my gratitude to my promotor Marthe De Boevre for her support and for giving me this amazing chance to study abroad.

Next, I want to thank Prof. Chiara Dall'Asta for letting me work in her lab. As well as for giving me all these interesting insides into my research topic.

Furthermore, I want to thank my supervisors Federico Ferrari and Raquel Torrijos for their useful feedback on my writing and their help during the practical aspects of my thesis.

I also want to thank my roommate and travel buddy Marie for joining me on this exciting once-in-a-lifetime adventure to Italy.

I want to give a special thanks to Clara for her loving encouragement, mental support and for making this Erasmus experience unforgettable.

Last but not least, my parents for their endless emotional and financial support as well as their love. As well as for allowing me to embark on this Erasmus adventure.

TABLE OF CONTENTS

LIST OF ABBREVIATIONS

ACN: Acetonitrile

AFB1: Aflatoxin B1

AFB2: Aflatoxin B2

AFB2A: Aflatoxin B2A

AFG1: Aflatoxin G1

AFG2: Aflatoxin G2

AFH1: Aflatoxin H1

AFL: Aflatoxicol

AFM1: Aflatoxin M1

AFM2: Aflatoxin M2

AFP1: Aflatoxin P1

AFQ1: Aflatoxin Q1

AFTs: Aflatoxins

AUC: Area Under the Curve

A_w: Water activity

BEA: beauvericin

CCS: Collision Cross Section

CE: Collision Energy

CYP 450: Cytochrome P450

DNA: Desoxyribonucleic acid

ECD: Electron Capture Detector

ESI: Electrospray ionization

ELISA: Enzyme-linked immunosorbent assay

EU: European Union

FID: Flame Ionization Detector

GAP: Good Agricultural Practices

GC: Gas Chromatography

HCC: Hepatocellular carcinoma

HPLC: High-Performance Liquid Chromatography

IMS: Ion Mobility Spectrometry

IM-MS: Ion Mobility-Mass Spectrometry

LD: Lethal dose

LE: Liquid Extraction

m/z: Mass-to-charge ratio

ML: Maximum Levels

MS: Mass Spectrometry

MW: Molecular Weight

PTFE: Polytetra-fluorethylene

QQQ: triple quadrupole

QuEChERS: Quick Easy Cheap Effective Rugged and Safe

RASFF: Rapid Alert System for Food and Feed

R^2: Correlation coefficient

SFC: Supercritical Fluid Chromatography

TLC: Thin Layer Chromatography

TOF: Time Of Flight

1. INTRODUCTION

1.1 MYCOTOXINS

Mycotoxins are secondary metabolites from fungi. More than 300 different mycotoxins have already been discovered. Their major producers are the fungi members of three genera: *Aspergillus, Fusarium,* and *Penicillium.* These fungi generally grow in humid and warm environments. There are different types of mycotoxins: aflatoxins (AFTs), zearalenone, ochratoxins, trichothecenes, fumonisins, and patulin are some examples. They can be found in soil and can contaminate various foods such as nuts, spices, cereals, grains, and dried fruits. (1–5) They are also present in feed and other raw materials. (4,6) The contamination occurs naturally and can happen before, during, or after the harvest. (1) The carry-over effect of mycotoxin contamination from feed to animal-derived products such as milk and eggs is an extra hazard. (4) The detection and prevention of contamination with mycotoxins are important because they can cause high-risk health problems in humans and animals that ingest them. These health problems develop mostly because of the carcinogenic properties of some mycotoxins. But teratogenic, neurotoxic, hepatotoxic, immunotoxic, and nephrotoxic effects were also observed. The diseases caused by mycotoxin poisoning are generally called ‘mycotoxicosis’. (7)

Avoiding contamination of food and feed is almost not possible as food processing doesn’t destroy the mycotoxins. (4) The only way to limit their occurrence is by taking preventive measures during the growth, processing, handling, and storage of these foods. The presence of mycotoxins in crops is mostly dependent on the temperature, relative air humidity, and moisture content of their environment. (8) This is a higher challenge for countries with a tropical climate and underdeveloped countries in which farmers lack the right equipment and knowledge to prevent contamination. The European Union (EU) has one of the highest food safety standards in the world. Crops coming from outside of the EU are controlled at the border. The Rapid Alert System for Food and Feed (RASFF) is a notification platform set up by the EU for the quick exchange of information. They report that most of the notifications associated with mycotoxins are related to aflatoxin

contamination. (4,9) In the future, climate change is expected to have an impact on mycotoxin presence in Europe. A temperature rise of +2°C worldwide would increase the risk of aflatoxin contamination from low to medium in maize-producing European countries. This is due to the more favourable growth conditions of the mycotoxigenic fungi. (1,10) Of all mycotoxins, AFTs are the ones that affect our food and feed the most. And they are in this way our biggest health concern. (2)

A second reason to prevent contamination, other than global health, is to avoid big agricultural and economic losses. Economic losses occur due to food waste on one hand. Throwing away contaminated food can have devastating consequences for poor farmers in susceptible climates. On the other hand, has the effect of contaminated feed on the health of farm animals, such as cows, a big impact. Estimated is that each year about 25% of all crops worldwide are contaminated by mycotoxins. (4,7,11)

1.2 AFLATOXINS

Aflatoxins are mycotoxins and can be further categorised. From the more than 20 known different AFTs, the most common ones are aflatoxin B1 (AFB1), aflatoxin B2 (AFB2), aflatoxin G1 (AFG1), and aflatoxin G2 (AFG2). Aflatoxin M1 (AFM1) and aflatoxin M2 (AFM2) are also often present but are less common than the previous four. AFB1, AFB2, AFG1, and AFG2 are produced by fungi such as *Aspergillus flavus* and *Aspergillus parasiticus*. *A. flavus* is dominant in for example corn and cottonseed, and produces AFB1 and AFB2. *A. parasiticus* on the other hand is dominant in peanuts, and produces AFG1, AFG2, AFB1, AFB2 and AFM1. Both fungi are known to grow at temperatures ranging from 12 to 41°C. The optimal growing temperature ranges from 25 to 32 °C. (2,7,12,13) In a study for *A. flavus* no growth is observed at a temperature of 20°C with a water activity (A_w) of 0.90. The optimal growth conditions on the other hand were found to be 30°C and an A_w of 0.99. (14)

The AFT biosynthesis consists of 18 steps which are conducted by enzymes. Acetyl coenzyme A is the starting point of this conversion into AFTs. The genes that code for

these enzymes and the biosynthetic regulation are numerous. At least 25 known genes have an impact. The main regulatory genes are aflR and aflS. A structural gene on the other hand is aflD. Both temperature and A_w influence gene expression. (2,5,15)

AFM1 and AFM2 are metabolites of respectively AFB1 and AFB2. They are formed through hydroxylation. (2,7,12) AFTs are heat-stable and can resist the temperatures used during food processing. Even temperatures higher than 100°C can be withstand. (16) The presence of AFB1 dominates and generally other AFTs such as AFB2, AFG1, and AFG2 do not occur without them. (7)

1.2.1 Toxicity

AFTs are mostly known for their hepatotoxicity. The ingestion of AFTs is followed by absorption into the blood and eventually first-pass metabolism in the liver by CYP450 enzymes. This leads to the formation of toxins. The CYP450 enzymes are mostly present in the liver, which shows why the liver is the most affected organ by mycotoxin poisoning. (12) Worldwide chronic poisoning is the biggest problem as acute AFT poisoning rarely happens. Only in some developing countries acute poisoning occurs. Symptoms are vomiting, pulmonary and cerebral edema, abdominal pain, and convulsions but also coma and death. (2,4) This is why it mostly causes long-term health effects. AFB1 was listed as a Group 1 carcinogen by the International Agency for Research on Cancer (IARC). AFM1 on the other hand used to be classified in Group 2B (‘possibly carcinogenic’) but was also put in Group 1 after further investigation. Substances in Group 1 are considered to be ‘carcinogenic to humans’. AFTs are also toxic to different animal species. The LD_{50} values of AFTs range from 0.5 to 10 mg/kg bodyweight depending on what kind of animal. This is the amount of a substance that is lethal to 50% of a group of test animals. The diseases caused by aflatoxin poisoning are collectively called ‘aflatoxicoses’. (4,7,17–19)

1.2.2 Chemical properties

AFTs are bisfuranocoumarin compounds. They consist of a bifuran ring fused with a coumarin group. The AFBs are different from AFGs as they have a pentanone ring instead of a lactone ring. AFTs have a low water solubility, namely 10-20 mg/l. They are soluble in polar organic solvents such as methanol, and acetonitrile and insoluble in non-polar solvents. AFTs have a high fluorescence in ultraviolet light. AFB1 and AFB2 get their name from reflecting blue light. The ‘G’ in AFG1 and AFG2 on the other hand refers to green fluorescence. AFM1 has blue-violet fluorescence. ‘M’ in AFM1 doesn’t stand for its fluorescence but refers to ‘milk’ as this is where AFM1 mostly occurs. All AFTs absorb UV light in a range of 362-363 nm. AFTs treated with ammonia at high temperatures and under high pressure, result in the opening of the lactone ring and decarboxylation. This lactone ring makes AFTs sensitive to alkaline hydrolysis. (2,5,7,12,20)

1.2.3 Legislation

AFT- levels are strictly regulated due to their high potency. The European Union sets low tolerance limits for AFT contaminations in food intended for human consumption. (21) In peanuts and processed products thereof, they set maximum levels (MLs) for AFB1 and the sum of AFB1, AFB2, AFG1, and AFG2. (12) For AFB1 the upper limit is 2 µg/kg. The upper limit for AFB1, AFB2, AFG1, and AFG2 combined is 4 µg/kg. This is very strict as for humans the safe limit lies between 4 and 30 µg/kg. (4,5,21) Most countries outside of the EU uphold similar regulations. Except for 13 countries that are known to not have any regulations and about 50 countries that don’t have any available data. Most of these countries are situated in Africa. Which makes importing from outside of the EU more difficult and associated with more risk. (22) For AFB1 extra regulations are made and other MLs are set for baby food and dietary foods for special medical purposes. In the case of raw milk, heat-treated milk, and milk-based products, extra regulations are necessary because ruminants who eat contaminated feed metabolise AFB1 to AFM1 and excrete this into their milk. In these cases, MLs are set for AFM1. The products are not allowed to be placed on the market when these MLs are exceeded. These rules and MLs are included in Commission Regulation (EC) No 1881/2006 of 19 December 2006 Article 1 and Article 12. Extra regulations are necessary for the import of these food products from third-world

countries. As their regulations involving AFTs might not be as strict. These regulations are described in Commission Regulation (EC) No 669/2009, Commission Implementing Regulation (EU) No 884/2014, and others. (12)

1.2.4 Control strategies

The many negative effects of AFT exposure ask for strict measures to reduce the contamination of food and feed. This contamination can occur during many stages of the food production process. From the farmer until the point of sale, everyone should be informed and stimulated to participate in limiting AFT production. Following good agricultural practices (GAPs), good manufacturing practices (GMPs), and good storage practices (GSPs) can help reduce contamination. Farmers can take post- and preharvest measures. Examples of pre-harvest strategies are the use of genetically modified crops with fungal resistance to for example *A. flavus*, the use of harmless fungi that compete with AFT-producing fungi, and proper and adequate irrigation of the fields to control kernel moisture. Postharvest practices, on the other hand, can be: drying the nuts properly, removing the visually damaged nuts while sorting, and controlling transport and storage conditions. Practically, mostly postharvest measures are used for AFT contamination prevention in peanuts. As the contamination usually gets worse during this stage of production and handling. (5,21,23–25)

1.2.5 The different aflatoxins

1.2.5.1 AFB1

AFB1 has a molecular formula $C_{17}H_{12}O_6$ and a molecular weight (MW) of 312.3 g/mol. The chemical structure is shown in Figure 1.1. (12) It is considered to be the most potent and most carcinogenic AFT. It is also known to be highly genotoxic. Other toxic effects include growth suppression, malnutrition, and modulation of the immune system. Studies have shown a link between AFB1 and the development of hepatocellular carcinoma (HCC) in animals and humans. (1) The toxic effects occur because of DNA-adduct formation and binding of the bioactivated AFB1-8,9-epoxide to mitochondrial and nuclear

macromolecules. The induction of oxidative stress is another way to reach toxic effects. This oxidative stress can compromise the AFB1 detoxification pathway. (4,12) AFB1 is heat resistant to a broad range of temperatures, including those used in food processing. This adds to its dangerous effects and the focus on preventing contamination with AFB1. (2)

The metabolization of AFB1 is shown in Figure 1.2. AFB1 can be metabolised into AFM1 and aflatoxin Q1 (AFQ1) through hydroxylation of respectively C_4 and C_{22}. Aflatoxin B2A (AFB2A) is formed by hydration of the double bond between C_2 and C_3. Epoxidation of the double bond between C_2 and C_3 results in aflatoxin B1- epoxide. Aflatoxin P1 (AFP1) is the result of o-demethylation. All previous metabolites are formed out of AFB1 through CYP450 enzymes. Only aflatoxicol (AFL) is not produced by CYP450 enzymes but by a soluble cytoplasmatic reductase enzyme system. The most carcinogenic and main AFB1-metabolite is AFM1. (7)

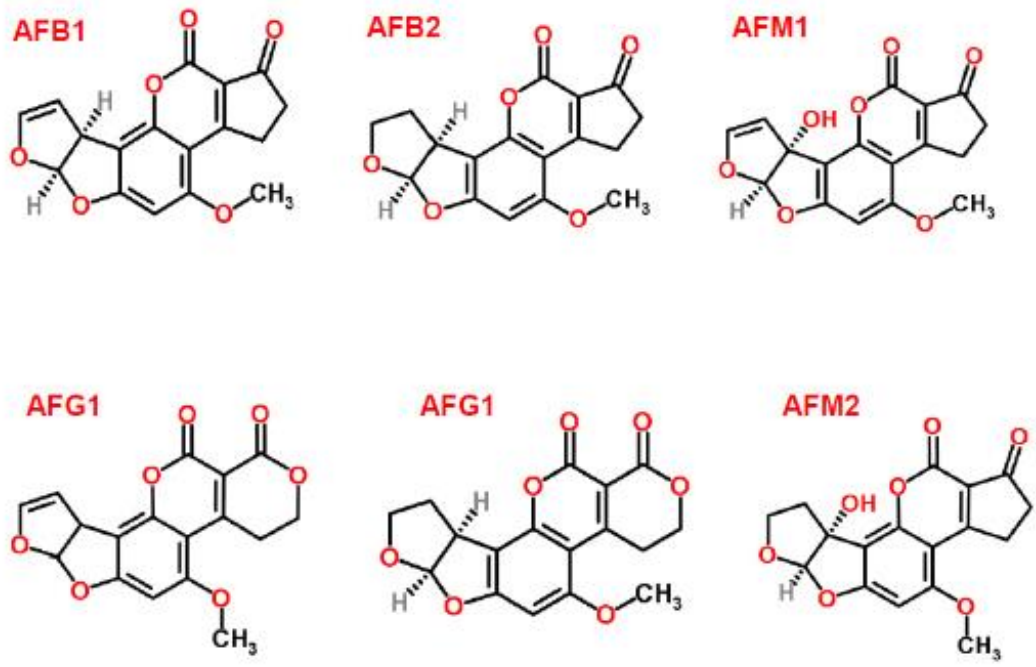

Figure 1.1: Chemical structures of aflatoxins (4)

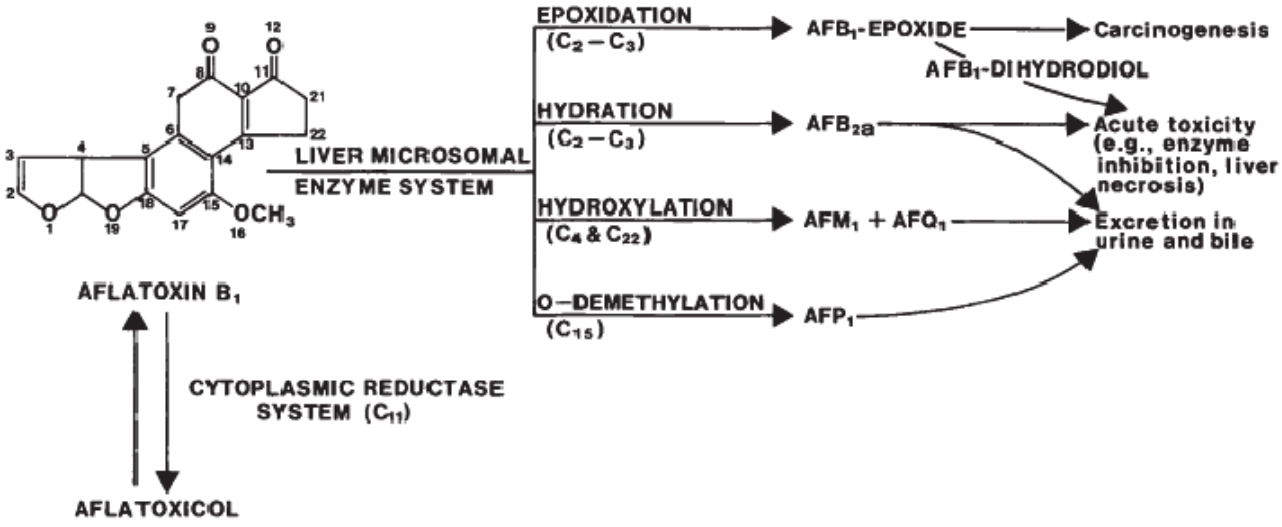

Figure 1.2: Metabolism of aflatoxin B1 in the liver. (7)

1.2.5.2 AFB2

$C_{17}H_{14}O_6$ is the molecular formula of AFB2 which corresponds with a molecular weight (MW) of 314.3 g/mol. This is slightly higher than the MW of AFB1 due to the loss of a double bond. AFB2 is the dihydro-derivative of AFB1. The chemical structure is shown in Figure 1.1. AFB2 can be hydroxylated into AFM2 by CYP450 enzymes. Fewer studies have been done on this aflatoxin. It is known that, different from for example AFB1, it cannot form the 8,9-epoxide as a metabolite. This explains why it is less toxic than AFB1 and AFG1. (2,12)

1.2.5.3 AFG1

$C_{17}H_{12}O_7$ is the molecular formula of AFG1. The molecular weight is 328.3 g/mol. (12) AFG1 is considered to be the second most toxic aflatoxin after AFB1. The chemical structure is shown in Figure 1.1. This aflatoxin can only be produced by *A. parasiticus.* (2,26) This AFT can be metabolised into its 8,9-epoxide. This epoxide can bind to DNA and other macromolecules in the body. (2,12)

1.2.5.4 AFG2

$C_{17}H_{14}O_7$ is the molecular formula of AFG2. The corresponding MW is 330.3 g/mol and is slightly higher than the MW of AFG1 due to the loss of a double bond. AFG2 is the dihydro-derivate of AFG1. The chemical structure is shown in Figure 1.1. (12) This aflatoxin can only be produced by *A. parasiticus.* (2,26) Out of this AFT, similar to AFB2, the 8,9-epoxide metabolite cannot be formed. (12)

1.2.5.5 AFM1

AFM1 is formed out of AFB1 through CYP1A2 metabolization in mammals. Namely hydroxylation of C_4 of the furan ring. This results in a slightly higher solubility. The log P decreases from 1.23 for AFB1 to 1.21 for AFM1. AFM1 has a molecular formula of $C_{17}H_{12}O_7$ and a molecular weight of 328.3 g/mol. The chemical structure is shown in Figure 1.1. (12,27)

AFM1 occurs in milk, blood, urine, … of humans and dairy cattle. The ingestion of food derived from this milk can also lead to exposure as AFM1 is heat stable and not affected by the processing of the milk. From 12 to 24 hours after cows consume contaminated feed, AFM1 is detectable in their milk. A correlation between the amount of AFB1 in the feed and the concentration of AFM1 in the milk is observed. This means that reducing AFB1 contamination of feed by using good agricultural practices (GAP) is the most effective way to limit AFM1 milk concentrations. (4,16) AFM1 can also be produced in very small amounts by the fungi itself. This is observed by the presence of AFM1 in for example corn. (27)

Its carcinogenic effect is created through the binding of AFM1 to DNA and the formation of an N7 guanine adduct. It is less mutagenic and less carcinogenic than AFB1 but has high genotoxicity. Other damaging effects of this AFT are liver damage, decreased milk production, anemia which results in a decrease of oxygen supply to the tissues, immunity suppression, and many others. (2,12)

1.2.5.6 AFM2

AFM2 is a CYP1A2 metabolite of AFB2 and is formed through metabolization in mammals. The metabolization of AFB2 is hydroxylation of the C_4 of the furan ring. This results in a more soluble metabolite. The log P decreases from 1.45 for AFB2 to 1.16 for AFM2. It has a MW of 330.3 g/mol and the molecular formula is $C_{17}H_{14}O_7$. The chemical structure is shown in Figure 1.1. (12) AFM2 can be found in organic fluids such as milk. (20)

1.3 PEANUTS AND MYCOTOXINS

Peanut (*Arachis hypogaea* L.) is a legume and is grown in soil. It is an important, popular, and affordable food source. It contains many useful nutrients such as vitamins, minerals, proteins, lipids, fibre, and carbohydrates. Peanuts are a critical part of the human diet in poorer countries where animal proteins are not as accessible to everyone. The reason is that it contains all the human essential amino acids. Peanuts also have been associated with reduced risk of diabetes, obesity, high blood pressure, and others. (23,28–30)

The first mycotoxins were discovered at the beginning of the 1960s. (21) They were discovered through the disease called turkey X disease, which is caused by AFT contamination of turkey feed. This feed consisted of groundnut meal imported from Brazil. The poisoning caused inflammation and necrosis to respectively the intestines and the liver of the turkeys. This led to turkeys showing severe signs of intoxication and even to an early death (1,8) From this, we can conclude that the contamination of peanuts has been a long-lasting problem and health concern. (21)

Peanuts are an important source of nutrition in for example many African countries. Peanuts are also popular as infant food. (31) Not only are they consumed raw but they are also present in foods such as cooking oils, peanut butter, and as weaning food for children. Undernutrition amongst children younger than five is a big problem in countries in Sub-

Saharan Africa as is the cause of almost half of the deaths below that age. Contamination with fungi and toxins plays a big part in this. Several theories of how AFT exposure results in malnutrition have been proposed. One of them is the damaging effect of AFTs on the intestinal tract. This results in an impaired barrier function and malabsorption. This can lead to zinc deficiency. A lack of zinc results in immune system dysfunction and growth faltering. To this day it is not very clear how AFT exposure leads to malnutrition as many other mechanisms have been proposed (23)

The AFT contamination of peanuts occurs due to the invasion of the nuts by fungi that produce aflatoxins. (21) Peanuts are the ideal substrate for the growth of fungi as they have a high nutritive value. *A. flavus* and *A. parasiticus* are the aflatoxigenic fungi that dominate in peanuts. These fungi are mostly present in humid and hot climates, the same regions where peanuts are produced. (23,32)

Contamination can take place in different stages of the production process. Namely during the growth, harvest, processing, and storage of the nuts. Aflatoxin contamination occurring before the harvest is associated with late-season drought as peanuts begin to dehydrate in the soil due to heat and lack of water. Post-harvest contamination is another possibility, this occurs when the nuts are not quickly dugs out, dried, and maintained at a safe moisture level. (21) In some countries peanuts are peeled by hand. Which can be time-consuming and painful for the hands. To ease this, peanuts are sometimes soaked in a water bad to soften the shell. Afterwards, the nuts are not dried but just stored wet. This high moisture level works fungi proliferation and aflatoxins production in hand. (23)

This shows the need for efficient and fast analysing techniques of AFTs in peanuts. Considering peanuts are an important and healthy food source in big parts of the world. As well as aflatoxins being a big threat to human and animal health.

1.4 DETECTION OF AFLATOXINS

Due to the major health problems that can occur from mycotoxin ingestion, many methods have been developed to detect and analyse them. These analyses can be performed on food and feed. In this way, it can be determined which foods are safe and which are not. As well as determining which foods are susceptible to AFT contamination.

1.4.1 Methods for detection

Examples of methods for analysing AFTs are high-performance liquid chromatography (HPLC) coupled with MS, FLD, UV, or DAD for detection; thin layer chromatography (TLC); gas chromatography (GC) coupled with MS, FID, or ECD detection; enzyme-linked immunosorbent assays (ELISA). The use of ELISA for analysing aflatoxins is not optimal as cross-reactivity with metabolites of the analytes or matrix components can occur. HPLC coupled with FLD (fluorescence detection) or UV (ultraviolet) detection is not commonly used anymore as these methods need extensive sample preparation and pre- or post-column derivatisation steps. Recently, the standard method for analysing mycotoxins in food has become HPLC coupled with mass spectrometry (MS). Depending on the matrix this can be triple quadrupole (QQQ) MS instruments enabling tandem mass spectrometry (MS/MS) or high-resolution mass spectrometry. These methods eliminate the need for sample derivatisation which is for example used for the enhancement of the fluorescence activity. Most of the time, sample preparation and extraction of the AFTs are still needed. (4,16,18,33)

1.4.2 HPLC-MS/MS

HPLC-MS/MS with ESI is the most used method nowadays to analyse AFTs and their metabolites. This works as follows. HPLC first divides the sample into chemical compounds. This is followed by MS. Firstly it ionizes the molecules. Afterwards, the molecules are identified and sorted according to their mass-to-charge ratio (*m/z*). The disadvantages of using LC-MS are that it is a very expensive method and that specialist expertise is necessary. The fact that the sensibility relies on ionization is another downside. This is due to unpredictable matrix effects caused by ESI ionization. The advantages, on

the other hand, are the low limit of detection and the possibility to analyse multiple mycotoxins at the same time. Using triple QQQ LC-MS/MS eliminates the use of the very expensive immuno-affinity clean-up columns. It also almost completely eliminates the probability of false positives. (4,16,18,33)

1.4.3 Ion Mobility–Mass Spectrometry coupled with TOF

Ion mobility-mass spectrometry (IM-MS) is ion mobility spectrometry (IMS) paired with mass spectrometry (MS). IM-MS is a technique that is based on the separation of the analytes based on size and mass. Both separation techniques are combined into one analytical platform. IM-MS is used for analysing small molecules as well as large protein complexes. (34) It can be used for non-targeted and targeted screening. Two things are required when this is used. First a database with collision cross section (CCS) values and second a database with accurate *m/z*-values. (35)

By using IMS, it is possible to determine the CCS values of different molecules. This value is a structural property of a molecule and can be used for, for example, identification. (36) Ion mobility determines CCS by deriving them from mobility values (K_0) using a physical model. This is done instead of directly measuring the surfaces of the molecules. Several studies have been executed and tables with the found CCS values have been published. (37)

IMS improves performance characteristics by reducing false detections this is done by enhancing the sensitivity, compound identification, and peak capacity. (36) The peak capacity is improved by adding a chromatographic separation before IM-MS-TOF. This enhances sensitivity. The chromatographic separation can be done by GC, supercritical fluid chromatography (SFC), and the most commonly used LC. (34) Any compound that is analysed using this, has 3 dimensions. Retention time (RT), molecular weight (MW), and drift time (DT). The RT is susceptible to different matrices. The RT of the AFTs can change when the matrix changes. DT and *m/z* on the other hand are independent of the matrix and

are only dependent on the nature and structure of the AFT. The DT is measured through a region filled with buffer gas, such as nitrogen, and put under an electric field. (36,37)

1.4.4 Sample preparation and extraction

Sample preparation and extraction are critical parts of letting the previously mentioned methods succeed. The goal of these steps leading up to the analysis is to eliminate sample matrix components that can interfere with the analytes of interest. In this case AFB1, AFB2, AFG1, and AFG2. This interference can happen during the ionization process and can cause signal suppression or enhancement. Steps that are often followed for pre-treatment are a liquid extraction (LE) step followed by some clean-up steps. These steps get rid of unwanted proteins, lipids, and sugars that are not of interest. For LE extraction, solvents such as acetonitrile (ACN), methanol, or mixtures of these two with each other, with water, and/or with organic acids are often used. (16,20)

Another extraction procedure that is commonly applied is the QuEChERS method. Which stands for Quick, Easy, Cheap, Effective, Rugged, and Safe method. This procedure starts with an extraction using acidified ACN. This is followed by the addition of salts and by a liquid-liquid partition of the analytes. Other techniques used for clean-up are liquid-liquid extraction (LLE), liquid-solid extraction (LSE), solid-phase extraction (SPE), or the expensive immunoaffinity columns which are highly selective. For each matrix, other clean-up steps can be the most efficient depending on their consistency. (16,20,38)

The criteria set for the analysis and sampling of AFTs by the EU are specified in Commission Regulation (EC) No 401/2006 of February 2006. (12) Over time, many studies have been done and a lot of progress has been made. However many difficulties such as complex food matrices or detection of low mycotoxin concentrations still occur. Further improvements to the existing analysing methods are needed. (4) The focus of this thesis is to improve the methods for analysing AFTs in the complex matrix of peanuts, especially the sample preparation and clean-up steps.

2. OBJECTIVES

The goal of this thesis is to evaluate the presence of multiple AFTs in Italian peanuts. This will be compared to data about AFT presence in peanuts from other countries such as Kenya and Zambia. The analysing will be done by an optimized QuEChERS-based method involving the triple quadrupole ultra-high-performance liquid chromatography tandem mass spectrometry (QQQ UHPLC-MS/MS). This is another goal of this thesis. Finding a more efficient and faster clean-up approach for peanut samples and the validation of this method. Peanuts are an important and healthy food source in big parts of the world. Aflatoxins are a big threat to human and animal health. Peanuts are easily affected by AFT contamination. But peanuts are a complex matrix and optimization of current existing methods is necessary.

Before starting practical work, multiple studies will be compared through literature study to find the best approach. The main focus is the sample preparation and extraction steps. Following this, the two most promising studies will be chosen to be performed experimentally. This will be done on blank peanut samples that are spiked with a standard AFT solution. This AFT solution contains the aflatoxins B1, B2, G1, and G2. These analytes will be the focus of this thesis. The samples will be prepared according to these two protocols. Afterwards, analysing will be done using triple QQQ UHPLC-MS/MS. The choice for the best clean-up approach will be made by comparing the recoveries and the efficiency. The chosen method will then be performed on the samples of interest, the nuts from Piacenza, Italy. These will first be screened for the presence of mycotoxins in the IM-MS-TOF. This will be done because ongoing research in the lab showed low concentrations of fungal isolates in the samples of interest. If the results of this screening are positive and AFTs are found, a more thorough analysis can be done with triple QQQ UHPLC-MS/MS. Our goal with the obtained data is to be able to make a statement about the contamination levels of peanuts grown in Italy compared to peanuts grown in other parts of the world.

3. MATERIALS AND METHODS

3.1 ‘dSPE’ APPROACH

3.1.1 Reagents and chemicals

Aflatoxin standard mixture of AFB1, AFB2, AFG1, and AFG2 was obtained from Sigma Aldrich (Stenheim, Germany)). Ultrapure water, acetonitrile, and formic acid were obtained from Scharlab Italia Srl (Milan, Italy). As salts (from VWR international) sodium chloride and anhydrous magnesium sulfate were used. As well as Z-sep^{+} and C18 sorbent. The mobile phase B consisted of methanol, water, and acetic acid (97:2:1 v/v). Mobile phase A was a 0.2 % acetic acid with 5 mM ammonium acetate solution. Methanol was used as phase C and ultrapure HPLC-graded water as phase D. (6) All solvents were obtained from Scharlab Italia Srl (Milan, Italy).

3.1.2 Sample information

The blank peanut samples for the determination of the right approach were obtained in a local supermarket in Bologna, Italy. The nuts were bought with shells. Before the start of the study, they were peeled and then ground in a cooking mixer until a fine and homogenous sample was obtained. The samples were then weighed and put into tightly closed vials. Afterwards, they were stored in a freezer at -18 °C until further use.

The peanut samples used in the final aflatoxin analysis came from Piacenza, Italy. They were ground and put into tubes before arriving in the lab. In total 30 different peanut samples arrived, harvested from ten different fields. Three samples came from each field. Once arrived they were kept in a freezer at -18°C until weighed. After weighing the nuts were kept in the fridge until further clean-up was performed.

3.1.3 Sample treatment

First 1 g of the homogenised ground peanuts was weighed and put into a 50 mL polypropylene centrifuge tube. To each tube, a spike concentration of 10 ppb aflatoxin standard mixture and 5 ml of water was added. To find the right approach a distinction

between spiking in the beginning and spiking at the end was made. After this, the tubes were put into a mechanical shaker for 10 minutes at 200 strokes/min. In this approach the QuEChERS method was followed. 5 ml of acetonitrile with 5 % formic acid solution, 2 g of magnesium sulfate, and 0.5 g of sodium chloride were added. Immediately after, the tubes were first shaken by hand and vortexed for approximately 30 seconds and then put into the centrifuge for 5 minutes at 3700*g*. After centrifuging, 1.5 ml of the upper layer was taken and transferred into a tube that contained 50 mg C18 and 50 mg Z-sep+. This was centrifuged again for 3 min at 1750*g*. 1.25 ml of the upper layer was taken and put into a clean vial. These vials were evaporated to dryness under a gentle nitrogen flow. When dry, the residue was reconstituted with 250 µl of mobile phase B and vortexed until there was no more residue left. (6)

3.2 'EASY' APPROACH

3.2.1 Reagents and chemicals

Aflatoxin standard mixture of AFB1, AFB2, AFG1, and AFG2 was obtained from Sigma Aldrich (Stenheim, Germany). A stock solution was made in acetonitrile. Acetonitrile, hexane, methanol (HPLC grade), and ultrapure water were obtained from Scharlab Italia Srl (Milan, Italy). The salts (from VWR international) used for the QuEChERS method were anhydrous magnesium sulfate and sodium chloride. Mobile phase A consisted of a 0.2% acetic acid solution with 5 mM ammonium acetate. Phase B on the other hand was a methanol/water/acetic acid solution (97:2:1 v/v). Methanol was used as phase C and phase D was ultrapure HPLC-graded water. (27) All solvents come from Scharlab Italia Srl (Milan, Italy).

3.2.2 Sample information

The peanuts samples were obtained and treated the same way as described in the 'dSPE' approach. This is described in chapter 3.1.2.

3.2.3 Sample treatment

As described in the (Sartori A. et al., 2014) study, 5 g of the homogenised ground peanuts were weighed into a 50 ml polypropylene centrifuge tube. To each tube, 100 ppb of the aflatoxin standard mixture and 10 ml ultrapure water were added. Half of the tubes were spiked in the beginning the other half was spiked in the end, right before filtering. Followed by 10 ml hexane and 15 ml acetonitrile. The tubes were then shaken in a mechanical shaker for 5 minutes at 200 strokes/min. In this approach, similar to the 'dSPE' approach the QuEChERS method was followed. In each tube, 4 g of magnesium sulfate and 1.5 g of sodium chloride were added, immediately followed by vortexing them for about 1 minute. Afterwards, the tubes were centrifuged for 7 minutes at 3000 rpm. After the phases are separated, 5 ml of the acetonitrile phase was taken out and put into a vial. These were evaporated to dryness under a gentle flow at room temperature. When completely dry, the residue was dissolved in 1.65 ml of a methanol/water (1:1 v/v) solution. At this point, another distinction was made to find the most efficient clean-up approach. Half of the samples spiked in the beginning, were filtered before injection (Di_1). The other half was not (Di_2). Idem for the samples spiked at the end (respectively Df_1 and Df_2). The filter used was a 0.22 µm PTFE (polytetrafluorethylene) filter. Half of all the samples were then put in the centrifuge again as an extra clean-up step. They were centrifuged for 5 minutes at 10000 rpm. (27)

3.3 LC-MS/MS INSTRUMENT

For the liquid chromatography analysis, a Thermo Scientific Dionex Ultimate 3000 instrument was used, coupled with a mass spectrometer (TSQ Vantage; Thermo Fisher Scientific). Separation was obtained with Kinetex column, 2.6 µm Evo C18, 100 x 2.1 mm, heated to 40 °C. 2 µl of each sample was injected and the flow rate was set up to 0.4 mL/min. Gradient elution was achieved by using water + 0.2 % acetic acid + 5 mM ammonium acetate (phase A) and methanol + 0.2 % acetic acid (phase B). Initially, A flow at 98% and B at 2%, for a minute, and then B to 90% in 8 min; constant gradient for 3 min until a rapid lowering of B back to the initial conditions after 13 min from start and kept for other 5 min before following injection. The total run time was 18 min. MS analysis was performed in positive ionization mode using SRM as a monitoring method, spray voltage,

capillary temperature, and sheath gas pressure. The following quantifier transitions were evaluated: AFB1 m/z 313.1>241.2 (CE 42eV), 313.1> 270.1 (CE 28eV), 313.1> 285.1 (CE 25eV); AFB2 m/z 315.2 > 259 (CE 30eV), 315.2 > 287 (CE 25eV); AFG1 m/z 329>243 (CE 25eV), AFG1 329>311 (CE 20eV); AFG2 m/z 331.3>245.3 (CE 25eV), AFG2 331.3>270 (CE 30eV), AFG2 331.3>285 (CE 30eV), AFG2 331.3>313.3 (CE 30eV). Calibration curves were set up using external standards (range 1 µg/Kg to 500 µg/Kg). Data acquisition was performed by Thermo Xcalibur 2.2 software (Thermo Fisher Scientific, Waltham, USA). (39)

3.4 MATRIX-MATCHED STANDARDS

Matrix-matched standards were used to evaluate both approaches. A calibration curve was made in a blank peanut matrix. This was done by spiking the blank matrix with a standard solution of AFB1, AFB2, AFG1, and AFG2 in acetonitrile. The spiked concentration ranged from 1 to 250 ppb in seven levels. This is needed in LC-MS/MS because the matrix can often suppress the signal of the analyte response. The calibration curve can be used as a reference and an accurate concentration of the aflatoxins can be interpreted.

For the screening in IM-MS-TOF, two different calibration curves were made. One calibration curve in purely solvent. The solvent is a mixture of 80 % methanol and 20 % water. The spiked AFT concentration ranged from 1 to 100 ppb in six levels. A second calibration curve was made like the calibration curve for the LC-MS/MS analyse. Namely in an uncontaminated blank peanut matrix. The concentrations range from 1 to 100 ppb in four levels.

3.5 COMPARISON OF BOTH STUDIES

The optimized ‘dSPE’ approach is compared to the optimized ‘EASY’ approach using AFT recoveries. The AFT recoveries of both clean-ups are calculated using this formula:

$$Recovery\ AFT\ (\%) = \frac{measured\ peak\ area\ for\ sample\ spiked\ in\ the\ beginning}{average\ measured\ peak\ area\ of\ samples\ spiked\ in\ the\ end} * 100 \quad (3.1)$$

Take sample 1.1 as an example this formula would then be:

$$Recovery\ AFT\ in\ sample\ 1.1\ (\%) = \frac{AUC\ Di\ 1.1}{AUC\ average\ Df\ 1} * 100$$

Di_1 and Di_2 are samples spiked with 100 ppb in the beginning, before performing any clean-up steps. Df_1 and Df_2 are samples spiked in the end, right before injection. All the Di_1 and Df_1 samples were put through an extra centrifuge step right before injection.

This calculation is performed for each sample. Afterwards, the recovery rates are analysed and compared with each other. Based on this, the decision is made about what the most accurate and most reliable method is.

3.6 IMS-TOF

The data of the screening were obtained using an ACQUITY UPLC I-Class system coupled to an ion mobility mass spectrometer Vion IMS QTOF. This system was operated in electrospray mode (ESI+). A reversed-phase C18 BEH column (Waters, UK) of 2.1×100 mm and a 1.7 µMm particle size, was used for the chromatographic separation. This column was heated at 35°C. The solvents used for LC were solvent A and solvent B. Solvent A was 1 mM ammonium acetate in water and solvent B was methanol. Both solvents were acidified with 0.5% acetic acid. To start the initial conditions (0.0−0.5 min) were set to 10 % solvent B. This increased over 3 min to 90% B. Next, it was put 1 min at 90% B. This was followed by reconditioning, achieved by 1.10 min of using the initial conditions. The total run time was 6 min. (36)

The MS detection was operated in the positive ESI mode and the mass range of *m/z* 50−1000. The following conditions were applied: for the positive ion mode, the capillary voltage was put at 0.5 kV. The cone voltage was put at 50 V, the source temperature at 150°C, the desolvation gas flow at 600 L/h, and the desolvation temperature at 450°C. Nitrogen was used as the collision gas. During the run two independent scans were alternatively conducted with different collision energies (CE) ($HDMS^E$ acquisition mode).

This acquisition mode is characterised by a low-energy scan of CE 6 eV. The low-energy scan is used to monitor the protonated/deprotonated molecules and other possible adducts. The high-energy scan (CE ramp 28-42 eV) on the other hand is used to fragment the through the collision cell traveling ions. (36)

The data was obtained using UNIFI software (Waters, UK). The Time-of-flight (TOF) analyser was used in the sensitivity mode. The analyse was conducted under the following conditions: the IMS gas (nitrogen) was put at a flow rate of 25 mL/min, the IMS pulse height at 45 V, and the wave velocity at 250 m/s. The acquisition rate was put at 10Hz. (36)

The used CCS database was the same as the one studied in (L. Righetti et al., 2020) (36) In this study was demonstrated that the found CCS-values were reproducible when using a similar type instrument by comparing the CCS-values with another IMS-QTOF instrument. The results of Vion # 1 were compared with Vion # 2 located in another lab. The interlaboratory reproducibility was proven. They also proved interplatform CCS reproducibility. This shows that the found CCS values can be used in different types of instruments without changing. (36) These values were also evaluated for four different matrices. The CCS values stayed constant for each AFT in a maize, wheat, rye, and malt matrix. (35)

4. RESULTS

4.1 PRELIMINARY TESTS USING UHPLC-MS/MS TRIPLE QUADRUPOLE

To find the best approach, multiple studies about QQQ UHPLC-MS/MS were taken into consideration and compared. With a focus on the clean-up step. The decision for the two most promising studies was made and performed on blank peanuts. The (Alsharif A. et al., 2019) (6) study, which is referred to as the 'dSPE' approach, and the (Sartori A. et al., 2014) (27) study, which is referred to as the 'EASY' approach. Both results are compared in the next chapters.

4.1.1 Blank peanuts

A blank peanut sample without a concentration spike was analysed using QQQ UHPLC-MS/MS. This was done to make sure that the peanuts from the supermarket in Bologna used as 'blank samples' are blank and had no traces of AFTs. UHPLC-MS/MS confirmed they were blank as the AUC could not be determent because there were no visible peaks found. The peanuts can be considered blank and are useful for making the calibration curves and comparing the two approaches.

4.1.2 Calibration curves

Table 4.1: The calculated correlation coefficient (R^2) and equations of the trendline of the calibration curve made in the blank matrix. The concentrations in this curve are 1 ppb, 5 ppb, 10 ppb, 25 ppb, 50 ppb, 100 ppb, and 250 ppb.

	R^2	Equations
AFB1	0.9987	y = 1593.3 x + 8484.2
AFB2	0.9999	y = 1312.6 x + 2142
AFG1	0.9986	y = 191.85 x + 1068.9
AFG2	0.9972	y = 270.98 x + 1982

The peak area (AUC) of each AFT was plotted in function of seven different AFT concentration levels. These levels of all four AFTs combined, ranging from 1 ppb to 250

ppb. The calculated R^2-values shown in Table 4.1 are all higher than 0.995. The equations all correspond with an increasing linear graph. This means that for a higher initial spike concentration, a higher peak area is observed. This is in line with what is expected.

4.1.3 'dSPE' approach

Table 4.2: Recovery (%) of the aflatoxins following the 'dSPE' approach.

	1.1[a]	1.2[a]	1.3[a]	2.1[b]	2.2[b]	2.3[b]
AFB1	49.26	51.40	52.80	63.81	68.32	72.07
AFB2	96.32	97.56	94.02	101.92	104.56	107.76
AFG1	55.29	55.44	58.23	71.61	79.03	75.06
AFG2	63.21	81.97	92.83	56.30	75.26	83.15

[a] samples were extra centrifuged one more time right before injection.

[b] samples were injected without an extra centrifuge step.

After following the 'dSPE' approach the samples were run in an UHPLC-MS/MS triple QQQ instrument. The recoveries (in %) of each AFT shown in Table 4.2 are calculated using formula 3.1. All samples were spiked with a concentration of 100 ppb standard AFT mix. Table 4.2 can be divided into two sides. On the left side, are the recoveries of the samples that went through an extra centrifuge step right before injection (1.1, 1.2, and 1.3). On the right side, the recoveries of the samples who didn't undergo this, are presented. namely 2.1, 2.2, and 2.3. For AFB1 the recoveries range from 49.26 % to 72.07 %. The recoveries calculated for the samples without the extra centrifuge step are significantly lower. This trend is also seen for other AFTs, except for AFG2. For AFB2 the recoveries lay between 94.02 % and 107.76 %. Recoveries for AFG1 range from 55.29 % to 79.03 %. AFG2 recoveries start at 56.30 % and go to 92.83 %.

4.1.4 'EASY' approach

Table 4.3: Recovery (%) of the aflatoxins following the 'EASY' approach with filter.

	1.1[a]	1.2[a]	1.3[a]	2.1[b]	2.2[b]	2.3[b]
AFB1	99.32	116.53	114.22	98.91	95.63	94.11
AFB2	119.13	124.44	114.74	109.66	99.28	95.63
AFG1	121.58	132.29	122.97	104.41	99.16	99.27
AFG2	124.05	137.35	125.20	110.78	99.87	94.36

[a] samples went through an extra centrifuge step right before the injection

[b] samples were injected without an extra centrifuge step

After following the 'EASY' approach the samples were run in a UHPLC-MS/MS triple quadrupole instrument. The recoveries (in %) of each AFT shown in Table 4.3 are calculated using formula 3.1. All samples were spiked with a concentration of 100 ppb standard AFT mix. Table 4.3 contains the data of the samples that were filtered with a 0.22 µm PTFE filter after the reconstitution and right before injection. The table can be divided into two sides. On the left side, the recoveries of samples 1.1, 1.2, and 1.3 can be found. These samples went through an extra centrifuge step right before injection. On the right side, the samples that didn't undergo this extra centrifuging can be seen, namely samples 2.1, 2.2, and 2.3. Most calculated recoveries are higher than 100 %. For AFB1 the recoveries range from 94.11 % to 116.53 %. The ones without the extra centrifuge step are a little lower. This trend is also visible for the other AFTs. For AFB2 the recoveries lay between 95.63 % and 124.44 %. Recoveries for AFG1 range from 99.16 % to 132.29 %. AFG2 recoveries start at 94.36 % and go to 137.35 %.

Table 4.4: Recovery (%) of the aflatoxins following the 'EASY' approach without filter.

	1.1[a]	1.2[a]	1.3[a]	2.1[b]	2.2[b]	2.3[b]
AFB1	121.28	105.33	94.49	121.84	119.99	116.30
AFB2	89.98	83.20	91.49	83.45	95.29	99.89
AFG1	98.34	91.64	98.70	95.57	105.56	102.99
AFG2	127.00	116.21	111.74	117.91	146.74	136.26

[a] samples went through an extra centrifuge step right before injection.

[b] samples were injected without an extra centrifuge step.

The recoveries (in %) of each AFT shown in Table 4.4 are calculated using formula 3.1. All samples were spiked with a concentration of 100 ppb standard AFT mix. Different from the results obtained in Table 4.3 these samples were not filtered. Table 4.4 can also be divided into two sides. On the left side, the recoveries of samples 1.1, 1.2, and 1.3 can be found. These samples went through an extra centrifuge step right after filtering and right before injection. On the right side, the samples that didn't undergo this extra centrifuging can be seen, namely samples 2.1, 2.2, and 2.3. Most calculated recoveries lay between 80 and 120 %. For AFB1 the recoveries range from 94.49 % to 121.84 %. For AFB2 the recoveries lay between 83.20 % and 99.89 %. Recoveries for AFG1 range from 91.64 % to 105.56 %. AFG2 recoveries start at 111.74 % and go to 146.74 %.

4.2 SCREENING USING IM-MS-TOF

4.2.1 Calibration curves

4.2.1.1 Calibration curves in solvent

Table 4.5: The calculated correlation coefficient (R^2) and equations of trendline of the calibration curve made in methanol: water (80:20 v/v). The concentration levels are 1 ppb, 5 ppb, 10 ppb, 25 ppb, 50 ppb, and 100 ppb.

	R^2	Equations
AFB1	0.9973	y = 6167.4 x + 16420
AFB2	0.9983	y = 7190.7 x + 18809
AFG1	0.9951	y = 8767.1 x + 34125
AFG2	0.9958	y = 8662.5 x + 29837

The peak area (AUC) of each AFT was plotted in function of six different AFT concentration levels. These levels of all four AFTs combined, ranging from 1 ppb to 100 ppb. The calculated R^2-values shown in Table 4.5 are all higher than 0.995. The equations all correspond with an increasing linear graph. This means that for a higher initial spike concentration, a higher peak area is observed. This is in line with what is expected.

In the next five tables (Table 4.6 until Table 4.10) data can be found about the *m/z*-values, the RT, and the CCS values of all four AFTs. And this is for each concentration level of the calibration curve made in solvent (methanol/water 80:20 v/v). Starting at an AFT concentration of 1 ppb and going until 100 ppb. The observed values are the ones determined by IM-MS-TOF in ESI^+ mode. The theoretical and expected values were found in databases of the IM-MS-TOF instrument. Delta CCS and the mass error were calculated by the software of the instrument itself. The delta RT was calculated by subtracting the observed RT from the expected RT.

Concerning the masses, the observed masses slightly differ from the expected masses. The differences are very little. This can be confirmed by the calculated mass errors. The difference is never bigger than 0.6 ppm.

For each AFT separately, the expected and the observed RTs lay very close together. Across the concentration range, the observed RTs are exactly the same. This is also the case for the expected RTs. All delta RTs are calculated to be 0.08 min. The RT is constant across all AFTs and the whole concentration range.

Lastly the CCS-values, across all concentrations the expected CCS is a constant for each AFT. The observed CCS always lay in a very close range of the expected values. This also shows in the delta CCS. These never exceed the value of 0.36 %.

Table 4.6: Data for the 1 ppb AFT spike in solvent. Data obtained through IM-MS-TOF analyse.

1 ppb	Theoretical mass (Da)	Observed mass (Da)	Mass error (ppm)	Expected RT (min)	Observed RT (min)	Δ RT (min)	Expected CCS ($Å^2$)	Observed CCS ($Å^2$)	Δ CCS (%)
AFB1	312.0634	312.0629	-0.4	7.01	6.93	0.08	163.15	163.14	0.01
AFB2	314.079	314.0784	-0.6	6.71	6.63	0.08	164.87	165.40	0.32
AFG1	328.0583	328.0577	-0.6	6.41	6.33	0.08	165.49	165.56	0.04
AFG2	330.0740	330.0734	-0.6	6.09	6.01	0.08	167.12	167.73	0.36

Table 4.7: Data for the 10 ppb AFT spike in solvent. Data obtained through IM-MS-TOF analyse.

10 ppb	Theoretical mass (Da)	Observed mass (Da)	Mass error (ppm)	Expected RT (min)	Observed RT (min)	Δ RT (min)	Expected CCS (Å^2)	Observed CCS (Å^2)	Δ CCS (%)
AFB1	312.0634	312.0629	-0.5	7.01	6.93	0.08	163.15	163.04	-0.07
AFB2	314.079	314.0785	-0.5	6.71	6.63	0.08	164.87	164.89	0.01
AFG1	328.0583	328.0578	-0.5	6.41	6.33	0.08	165.49	165.39	-0.06
AFG2	330.074	330.0734	-0.6	6.09	6.01	0.08	167.12	167.36	0.14

Table 4.8: Data for the 25 ppb AFT spike in solvent. Data obtained through IM-MS-TOF analyse.

25 ppb	Theoretical mass (Da)	Observed mass (Da)	Mass error (ppm)	Expected RT (min)	Observed RT (min)	Δ RT (min)	Expected CCS (Å^2)	Observed CCS (Å^2)	Δ CCS (%)
AFB1	312.0634	312.0629	-0.5	7.01	6.93	0.08	163.15	163.04	-0.07
AFB2	314.079	314.0785	-0.5	6.71	6.63	0.08	164.87	164.89	0.01
AFG1	328.0583	328.0578	-0.5	6.41	6.33	0.08	165.49	165.39	-0.06
AFG2	330.074	330.0734	-0.6	6.09	6.01	0.08	167.12	167.36	0.14

Table 4.9: Data for the 50 ppb AFT spike in solvent: Data obtained through IM-MS-TOF analyse.

50 ppb	Theoretical mass (Da)	Observed mass (Da)	Mass error (ppm)	Expected RT (min)	Observed RT (min)	Δ RT (min)	Expected CCS (Å^2)	Observed CCS (Å^2)	Δ CCS (%)
AFB1	312.0634	312.0629	-0.5	7.01	6.93	0.08	163.15	163.04	-0.07
AFB2	314.079	314.0785	-0.5	6.71	6.63	0.08	164.87	164.89	0.01
AFG1	328.0583	328.0578	-0.5	6.41	6.33	0.08	165.49	165.39	-0.06
AFG2	330.074	330.0734	-0.6	6.09	6.01	0.08	167.12	167.36	0.14

Table 4.10: Data for the 100 ppb AFT spike in solvent: Data obtained through IM-MS-TOF analyse.

100 ppb	Theoretical mass (Da)	Observed mass (Da)	Mass error (ppm)	Expected RT (min)	Observed RT (min)	Δ RT (min)	Expected CCS (Å^2)	Observed CCS (Å^2)	Δ CCS (%)
AFB1	312.0634	312.0629	-0.5	7.01	6.93	0.08	163.15	163.04	-0.07
AFB2	314.079	314.0785	-0.5	6.71	6.63	0.08	164.87	164.89	0.01
AFG1	328.0583	328.0578	-0.5	6.41	6.33	0.08	165.49	165.39	-0.06
AFG2	330.074	330.0734	-0.6	6.09	6.01	0.08	167.12	167.36	0.14

4.2.1.2 Calibration curves in blank matrix

Table 4.11: The calculated R^2-values and equations of the calibration curve made in blank matrix with the concentrations being 1 ppb, 10 ppb, 50 ppb, and 100 ppb.

	R^2	Equations
AFB1	0.9474	y = 3776.2 x + 78440
AFB2	0.9828	y = 25584 x + 176074
AFG1	0.9283	y = 5760.4 x + 119336
AFG2	0.9651	y = 29211 x + 261304

The peak area (AUC) of each AFT was plotted in function of four different AFT concentration levels. These levels of all four AFTs combined, ranging from 1 ppb to 100 ppb. The calculated R^2-values shown in Table 4.11 are all lower than 0.995. The equations all correspond with an increasing linear graph. This means that for a higher initial spike concentration, a higher peak area is observed. This is in line with what is expected.

In the next four tables (Table 4.12 until Table 4.15) data can be found about the *m/z*-values, the RT, and the CCS values of all four AFTs. And this is for each concentration level of the calibration curve made in matrix and solvent. Starting at an AFT concentration of 1 ppb and going until 100 ppb. The observed values are the ones determined by IM-MS-TOF in ESI^+ mode. The theoretical and expected values were found in databases of the IM-MS-TOF instrument. Delta CCS and the mass error were calculated by the software of the instrument itself. The delta RT was calculated by subtracting the observed RT from the expected RT.

Similar to what can be previously seen in chapter 4.2.1.1, the observed masses are slightly different from the expected masses. The differences are very little. This can be confirmed by the calculated mass errors. The difference is never bigger than 0.5 ppm.

For each AFT separately, the expected and the observed RTs lay very close together. Across the concentration range, the observed RTs are exactly the same. The RT is constant across all AFTs and the whole concentration range. All delta RTs are calculated to be 0.09 min. This is slightly longer than the delta RT seen in the samples with only solvent.

Lastly the CCS-values, across all concentrations the expected CCS is a constant for each AFT. The observed CCS always lay in a very close range of the expected values. This also shows in the delta CCS. These never exceed the value of 0.14 %. This difference is smaller than in the samples with only solvent.

Table 4.12: Data for the 1 ppb AFT spike in blank matrix and solvent: Data obtained through IM-MS-TOF analyse.

1 ppb	Theoretical mass (Da)	Observed mass (Da)	Mass error (ppm)	Expected RT (min)	Observed RT (min)	Δ RT (min)	Expected CCS (Å^2)	Observed CCS (Å^2)	Δ CCS (%)
AFB1	312.0634	312.0629	-0.5	7.01	6.92	0.09	163.15	163.1	-0.03
AFB2	314.079	314.0785	-0.5	6.71	6.62	0.09	164.87	164.85	-0.01
AFG1	328.0583	328.0578	-0.5	6.41	6.32	0.09	165.49	165.73	0.14
AFG2	330.074	330.0736	-0.4	6.09	6.00	0.09	167.12	166.91	-0.13

Table 4.13: Data for the 10 ppb AFT spike in blank matrix and solvent: Data obtained through IM-MS-TOF analyse.

10 ppb	Theoretical mass (Da)	Observed mass (Da)	Mass error (ppm)	Expected RT (min)	Observed RT (min)	Δ RT (min)	Expected CCS (Å^2)	Observed CCS (Å^2)	Δ CCS (%)
AFB1	312.0634	312.0629	-0.5	7.01	6.92	0.09	163.15	163.1	-0.03
AFB2	314.079	314.0785	-0.5	6.71	6.62	0.09	164.87	164.85	-0.01
AFG1	328.0583	328.0578	-0.5	6.41	6.32	0.09	165.49	165.73	0.14
AFG2	330.074	330.0736	-0.4	6.09	6.00	0.09	167.12	166.91	-0.13

Table 4.14: Data for the 50 ppb AFT spike in blank matrix and solvent: Data obtained through IM-MS-TOF analyse.

50 ppb	Theoretical mass (Da)	Observed mass (Da)	Mass error (ppm)	Expected RT (min)	Observed RT (min)	Δ RT (min)	Expected CCS (Å²)	Observed CCS (Å²)	Δ CCS (%)
AFB1	312.0634	312.0629	-0.5	7.01	6.92	0.09	163.15	163.1	-0.03
AFB2	314.079	314.0785	-0.5	6.71	6.62	0.09	164.87	164.85	-0.01
AFG1	328.0583	328.0578	-0.5	6.41	6.32	0.09	165.49	165.73	0.14
AFG2	330.074	330.0736	-0.4	6.09	6.00	0.09	167.12	166.91	-0.13

Table 4.15: Data for the 100 ppb AFT spike in blank matrix and solvent: Data obtained through IM-MS-TOF analyse.

100 ppb	Theoretical mass (Da)	Observed mass (Da)	Mass error (ppm)	Expected RT (min)	Observed RT (min)	Δ RT (min)	Expected CCS (Å²)	Observed CCS (Å²)	Δ CCS (%)
AFB1	312.0634	312.0629	-0.5	7.01	6.92	0.09	163.15	163.1	-0.03
AFB2	314.079	314.0785	-0.5	6.71	6.62	0.09	164.87	164.85	-0.01
AFG1	328.0583	328.0578	-0.5	6.41	6.32	0.09	165.49	165.73	0.14
AFG2	330.074	330.0736	-0.4	6.09	6.00	0.09	167.12	166.91	-0.13

4.2.2 Chromatograms

4.2.2.1 Chromatograms of AFB1

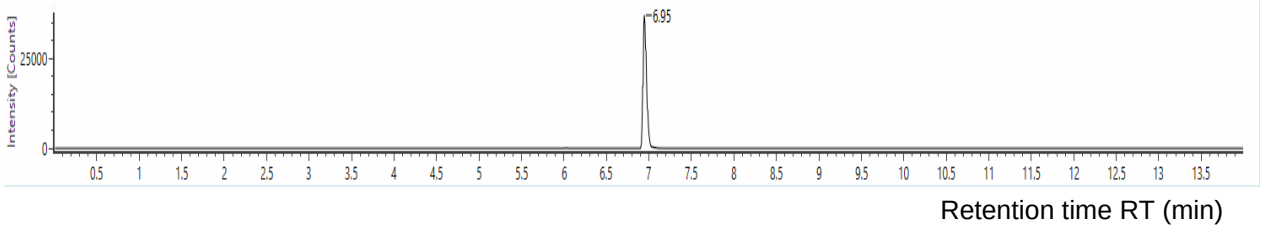

Figure 4.1: Chromatogram of AFB1 obtained through IM-MS-TOF analyse in the ESI⁺ mode. On the y-axis, the intensity (in counts) is shown and on the x-axis, the retention time RT (in min) is displayed.

The chromatogram in Figure 4.1 was obtained through IM-MS-TOF analyse of the sample spiked with 100 ppb AFT, operated in the ESI⁺ mode. For *m/z* 313.0704 Da is one

clear peak in the intensity visible at 6.95 minutes after the start of the run. This is the RT of AFB1. No other interfering peaks or noise can be seen.

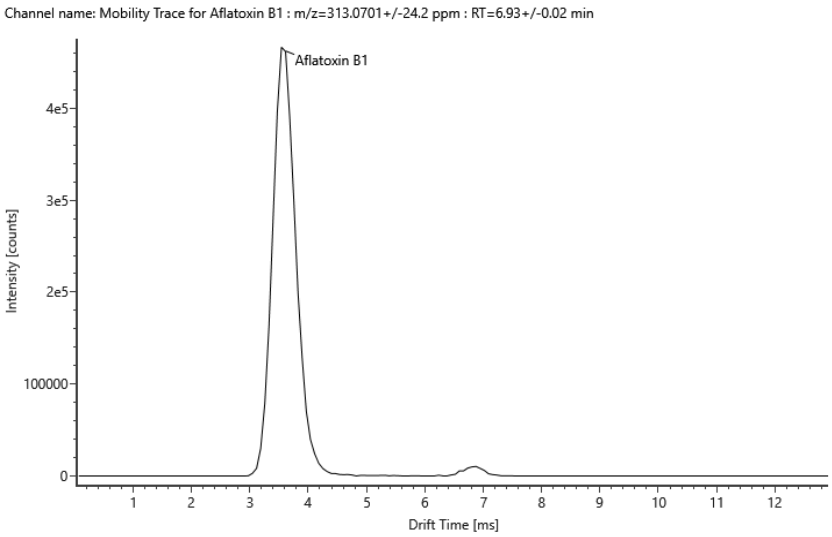

Figure 4.2: Chromatogram of AFB1 obtained through IM-MS-TOF analyse in the ESI$^+$ mode. On the y-axis, the intensity (in counts) is displayed and on the x-axis, the drift time DT (in ms) is shown.

The chromatogram in Figure 4.2 was obtained through IM-MS-TOF analyse of the sample spiked with 100 ppb AFT in the ESI$^+$ mode. For *m/z* 313.0704 Da and RT of +/- 6.93 min, one big peak and one small peak are visible in the intensity. This is based on the DT (in ms). Previously, based on the RT, these two separate peaks were not visible. The big peak comes from the protonated AFB1 form $[M + H]^+$. The small peak corresponds with the other formed adducts of AFB1, namely the sodium $[M + Na]^+$ and the potassium $[M + K]^+$ adduct.

4.2.2.2 Chromatograms of AFB2

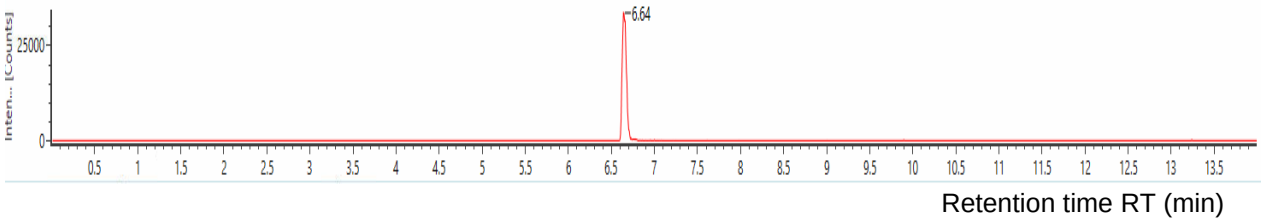

Figure 4.3: Chromatogram of AFB2 obtained through IM-MS-TOF analyse in the ESI$^+$ mode. On the y-axis, the intensity (in counts) is displayed and the x-axis shows retention time RT (in min).

The chromatogram in Figure 4.3 was obtained through IM-MS-TOF analyse of the sample spiked with 100 ppb AFT in the ESI$^+$ mode. For *m/z* 315.0861 Da, there is after 6.64 minutes of running one clear peak in the intensity visible. This is the RT of AFB2. No other interfering peaks or noise can be seen.

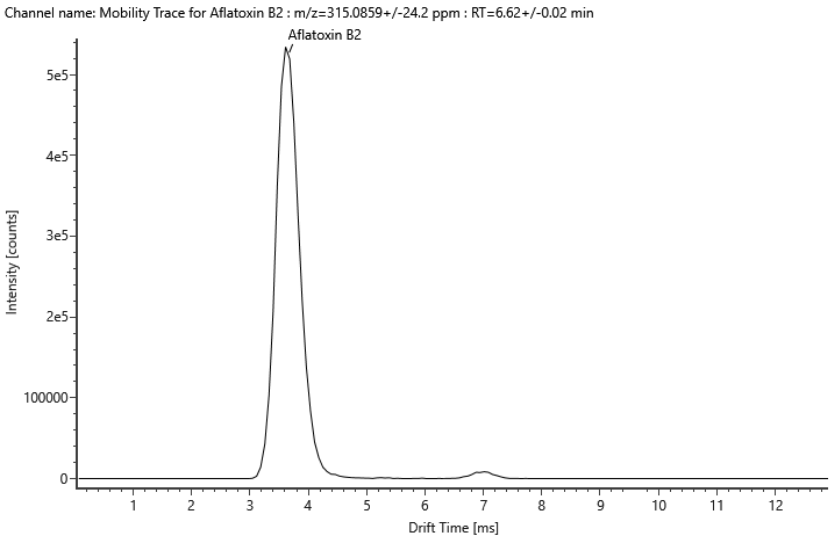

Figure 4.4: Chromatogram of AFB2 obtained through IM-MS-TOF analyse in the ESI$^+$ mode. On the y-axis, the intensity (in counts) is displayed and the x-axis shows the drift time DT (in ms).

The chromatogram in Figure 4.4 was obtained through IM-MS-TOF analyse of the sample spiked with 100 ppb AFT, operated in the ESI$^+$ mode. For *m/z* 315.0861 Da and RT of +/- 6.62 min, one big peak and one small peak are visible in the intensity. This is based on the DT (in ms). Previously, based on the RT, these two separate peaks were not visible. The big peak corresponds with the protonated AFB2 form $[M + H]^+$. The small peak comes from the other formed adducts of AFB2, namely $[M + Na]^+$ and $[M + K]^+$.

4.2.2.3 Chromatograms of AFG1

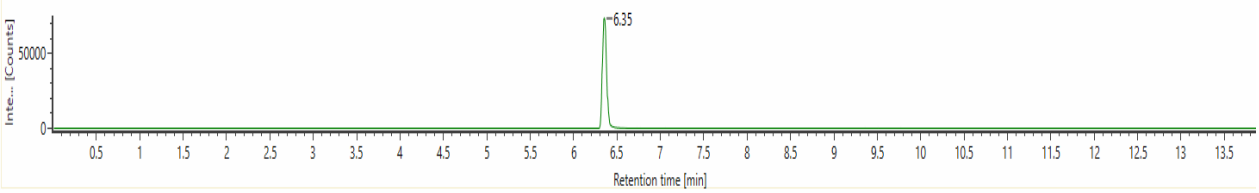

Figure 4.5: Chromatogram of AFG1 obtained through IM-MS-TOF analyse in the ESI⁺ mode. The y-axis displays the intensity (in counts) and the x-axis shows the retention time RT (in min).

The chromatogram in Figure 4.5 was obtained through IM-MS-TOF analyse of the sample spiked with 100 ppb AFT, operated in the ESI⁺ mode. For *m/z* 329.0653 Da, there is one clear peak in the intensity visible after 6.35 minutes of running. This is the RT of AFG1. No other interfering peaks or noise can be seen.

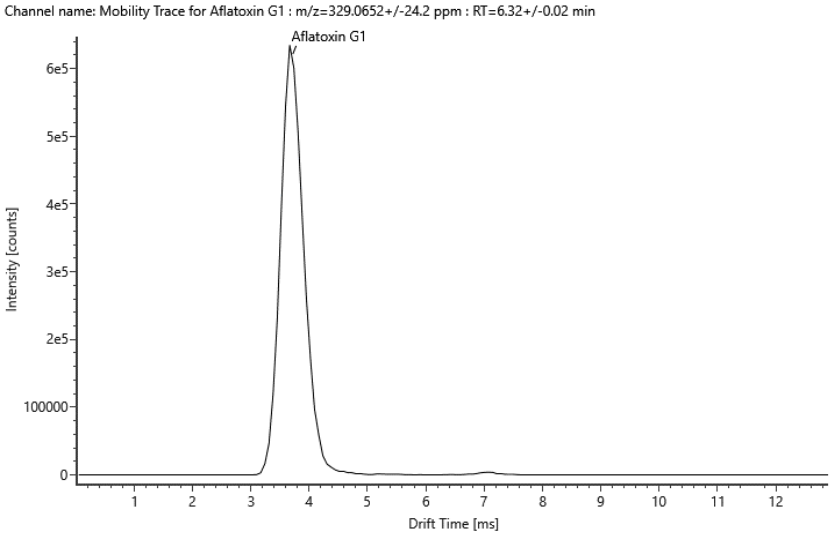

Figure 4.6: Chromatogram of AFG1 obtained through IM-MS-TOF analyse in the ESI⁺ mode. The y-axis shows the intensity (in counts) and the x-axis displays the drift time DT (in ms).

The chromatogram in Figure 4.6 was obtained through IM-MS-TOF analyse of the sample spiked with 100 ppb AFT, operated in the ESI⁺ mode. For *m/z* 329.0652 Da and RT of +/- 6.32 min, one big peak and one very small peak are visible in the intensity. This is based on the DT (in ms). Previously, based on the RT, these two separate peaks were

not visible. The big peak comes from the protonated AFG1 form $[M + H]^+$. The very small peak corresponds with the other formed adducts of AFG1, namely $[M + Na]^+$ and $[M + K]^+$.

4.2.2.4 Chromatograms of AFG2

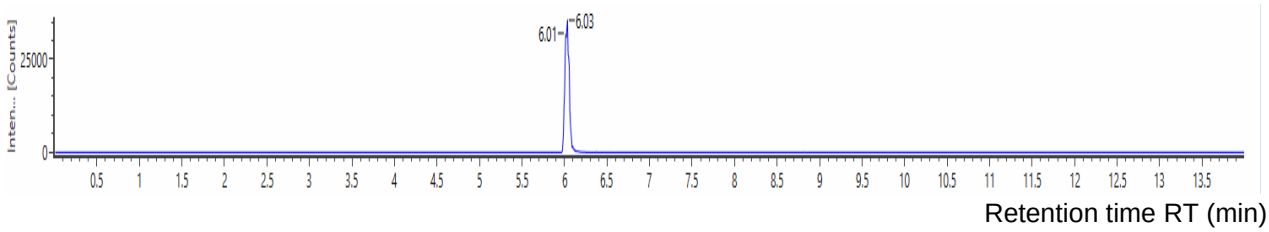

Figure 4.7: Chromatogram of AFG2 obtained through IM-MS-TOF analyse in the ESI$^+$ mode. The y-axis shows the intensity (in counts), and the x-axis displays the retention time RT (in min).

The chromatogram in Figure 4.5 was obtained through IM-MS-TOF analyse of the sample spiked with 100 ppb AFT in the ESI$^+$ mode. For *m/z* 331.0810 Da, there is one clear peak in the intensity visible after 6.03 minutes of running. This is the RT of AFG2. No other interfering peaks or noise can be seen.

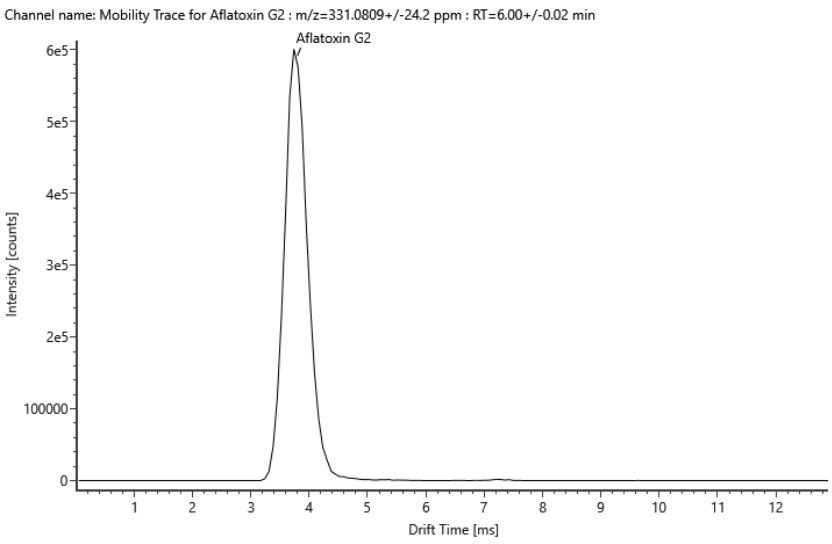

Figure 4.8: Chromatogram of AFG2 obtained through IM-MS-TOF analyse in the ESI$^+$ mode. The y-axis shows the intensity (in counts), and the x-axis displays the drift time DT (in min).

The chromatogram in Figure 4.8 was obtained through IM-MS-TOF analyse of the sample spiked with 100 ppb AFT, operated in the ESI^+ mode. For *m/z* 331.0810 Da and RT of +/- 6.00 min, one big peak and one very small peak are visible in the intensity. This is based on the DT (in ms). Previously, based on the RT, these two separate peaks were not visible. The big peak comes from the protonated AFG2 form $[M + H]^+$ and the small one corresponds with the other formed adducts of AFG2, namely $[M + Na]^+$ and $[M + K]^+$.

4.2.3 The mobility 3D-plots

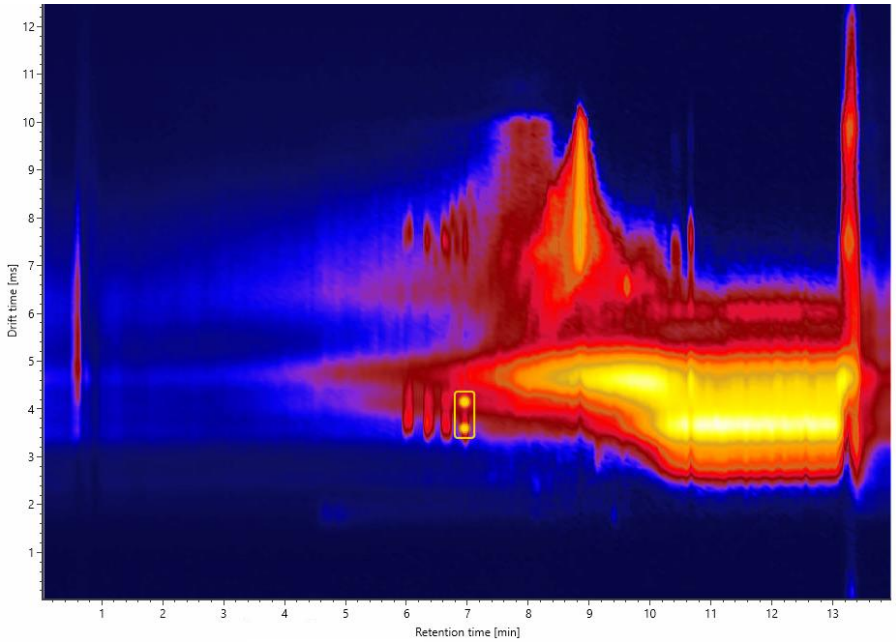

Figure 4.9: The 3D mobility plot of AFB1 obtained with IM-MS-TOF in the ESI^+ mode. The x-axis shows the RT (in min) and the y-axis displays the DT (in min).

In Figure 4.9 the 3D mobility plot of AFB1 is visible. The x-axis depicts the RT in minutes, and the y-axis the DT in ms. The two yellow dots have the same RT of around 7 minutes. This is the known RT of AFB1. The DT on the other hand is different for both forms. This shows that there are at least two different versions of AFB1 present. One of the points is AFB1 in its protonated form $[M + H]^+$, the other point is the potassium $[M + K]^+$ and sodium $[M + Na]^+$ adduct of AFB1 combined.

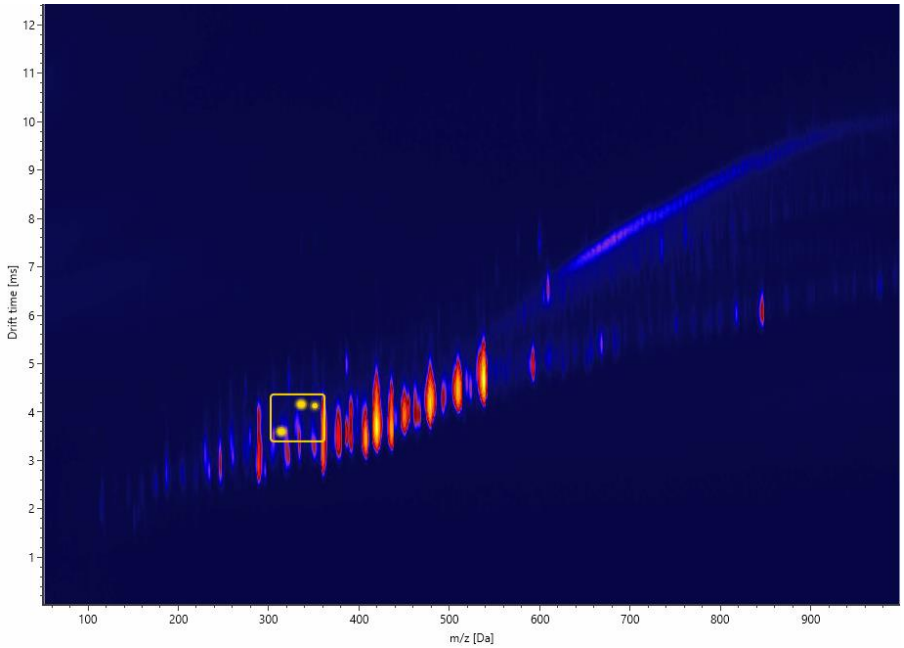

Figure 4.10: The 3D mobility plot of AFB1 obtained with IM-MS-TOF in the ESI$^+$ mode. The x-axis shows the m/z-values (in Da) and the y-axis displays the DT (in ms).

Figure 4.10 shows the 3D mobility plot of AFB1 with in the x-axis the *m/z*-values (Da) and the DT (ms) on the y-axis. For this the RT time was put at around 7 minutes, the found RT of AFB1 in figure 4.11. Three different yellow dots are visible. Two of them have the same DT but a different *m/z* value. This shows that there are multiple adducts of AFB1. The sodiated $[M + Na]^+$ and the potassium $[M + K]^+$ form.

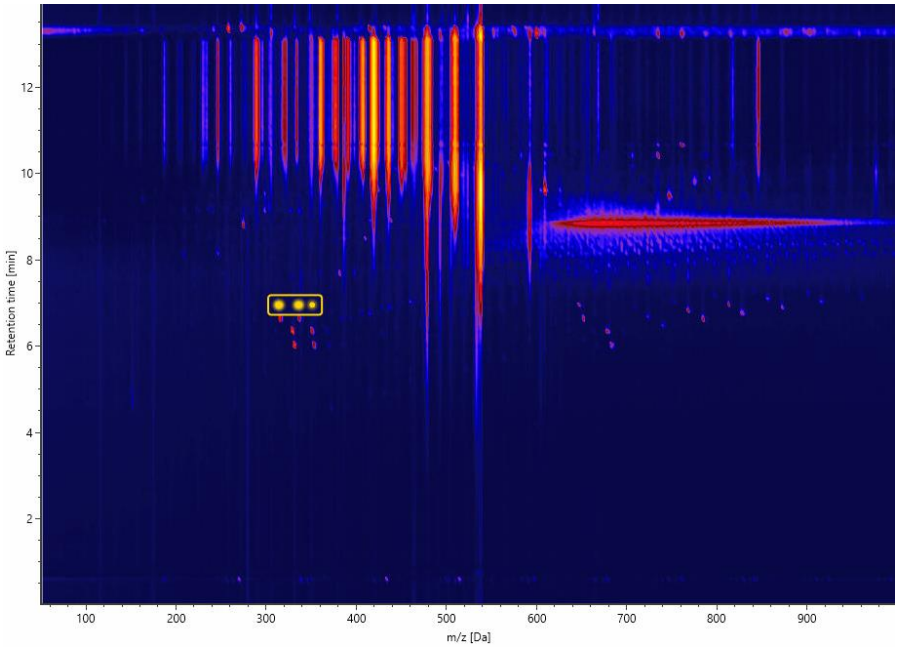

Figure 4.11: The 3D mobility plot of AFB1 obtained with IM-MS-TOF in the ESI$^+$ mode. The x-axis shows the m/z-values (in Da) and the y-axis displays the RT (in min).

The 3D mobility plot in Figure 4.11 displays *m/z* (in Da) in function of RT (in min). It shows three points with the same RT but 3 different *m/z*-values. This RT is around 7 min. All three *m/z*-values lay between 300 and 380 Da. This confirms what is seen in Figures 4.9 and 4.10: there are at least 3 different forms of AFB1. The protonated form $[M + H]^+$ and two adducts of AFB1, $[M + Na]^+$ and $[M + K]^+$

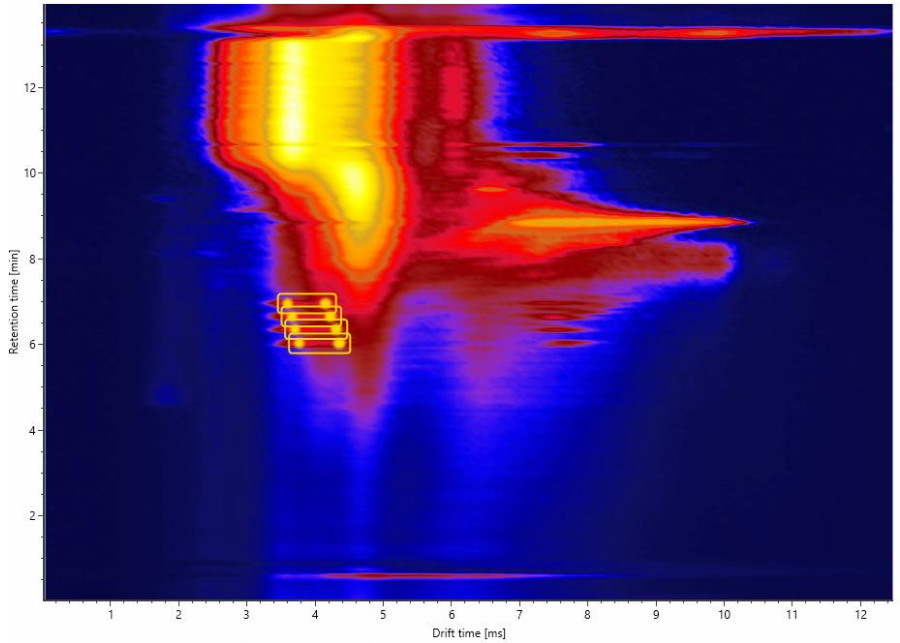

Figure 4.12: The 3D mobility plot of AFB1, AFB2, AFG1, and AFG2 obtained with IM-MS-TOF in the ESI$^+$ mode. The x-axis shows the DT (in ms) and the y-axis displays the RT (in min).

The 3D mobility plot in Figure 4.12 displays DT (in ms) in function of RT (in min). Eight different yellow points, at four different retention times (RT) can be seen. The retention times belong to the four AFTs. This plot shows an overview of the mobility of AFB1, AFB2, AFG1, and AFG2. From this plot it can be assumed that each AFT has a protonated and at least one other formed, this is shown by the two different drift times (DT).

4.2.4 The peanuts from Piacenza, Italy

The peanut samples of interest are the peanuts grown on the ten different fields in Piacenza, Italy. These nuts were screened on the occurrence of mycotoxins using IM-MS-TOF in the ESI$^+$ mode. All 30 samples were found to be blank. No peaks were observed for any of the AFTs. From this, we can conclude that the peanuts were probably not contaminated with AFB1, AFB2, AFG1, and AFG2. On the other hand, some traces of another mycotoxin were found, namely beauvericin (BEA).

5. DISCUSSION

5.1 PRELIMINARY TESTS USING UHPLC-MS/MS TRIPLE QUADRUPOLE

The main goal of these preliminary tests was to check if the recovery is still sufficient after the changes that were made to the original studies (6,27). The results of the mycotoxin analysis are checked to make sure they are still reliable. This is done by creating four kinds of differently-treated peanut samples. The Di_1 and Di_2 samples are spiked with 100 ppb in the beginning, before performing any clean-up steps. The Df_1 and Df_2 samples are spiked in the end, right before injection. These different samples are created to be able to calculate the recoveries. The Di_1 and Df_1 samples are put through an extra centrifuge step right before injection. In the next chapters, it is evaluated if adding these steps to the protocol would improve the clean-up and that they won't harm the results of the analysis.

5.1.1 Calibration curves

The strength of the association between two variables can be evaluated through to correlation coefficient R^2. In this calibration curve, these variables are the spiked AFT concentration and the measured peak area after analysis. R^2- values always lay between 0 and 1. Zero means no association and 1 corresponds with the highest association. (40) As displayed in Table 4.1, all the R^2-values are higher than 0.995. This means that the spiked concentration is strongly associated with the results of the QQQ UHPLC-MS/MS analyse, the AUC. It can be assumed that the peak area is related to the spike concentration. The calibration curve can now be used to determine the AFT concentrations when the AUC has been measured by the QQQ UHPLC-MS/MS.

5.1.2 'dSPE' approach

In this approach, some changes were made to the original study (6) to have a more efficient clean-up. The calculated recoveries are discussed in this chapter.

In Table 4.2 a clear decline in the recovery is visible for the samples that were purified with an extra centrifuge step (1.1, 1.2, and 1.3). This trend can be seen for all AFTs, except for AFG2. The samples without the extra centrifuge step lose less of the AFT concentration that is present. It can be assumed that the accuracy of the results of the analysis decline when this step is added to the protocol. The ideal recovery would be 100 %, this would mean that during the extraction and sample preparation, no AFTs were lost. An acceptable recovery range is 70 % to 110 %. (41) The recoveries of AFB1 and AFG1 for the samples with the extra centrifuge step lay far below 70 % and are not acceptable. Taking all this into consideration, the addition of the centrifuge step to the protocol makes the measurement of the AFT concentration less accurate. The true concentration and the observed concentration will be too far apart. This step will not be added to the protocol.

Looking at the right side of Table 4.2: The AFT recovery that is reached for samples 2.1, 2.2, and 2.3 using this approach is acceptable. The recoveries lay close to 70% or higher. This is sufficient as the acceptable recoveries range from 70% - 110%. (41) Only AFB2 has a recovery of more than 100 %. This is still acceptable as it is less likely to be a systematic mistake, caused by matrix effects, but more likely to be caused by accident. A possible reason for this could be adding a volume of the AFT spike solution that was too high. For the first sample of AFG2 (2.1), the recovery is a lot lower than 70 %. The rates of the second and third analyses are higher than 70 %. The rates differentiate a lot from each other, this could be due to a human mistake during the sample preparation. The trend that the recoveries are lower for the samples with the extra centrifuge step, is not visible for AFG2. The recovery values of AFG2 have a very wide range and no real consensus. To conclude, this approach could be an option for the real sample preparation of the analytes of interest, the Italian peanuts.

5.1.3 ‘EASY’ approach

The (Sartori A. et al., 2014) (27) protocol was followed but some changes were made in hopes of finding a more efficient clean-up.

In Table 4.3 most calculated recoveries are higher than 100 %. Almost all of them were significantly higher, exceeding the acceptable recovery range of 70% - 110%. (41) The recoveries from samples that went through the extra centrifuge step are a little higher than the ones that didn't. This trend is seen for all the AFTs. It is similar to what is observed in the 'dSPE' approach. The recoveries after the centrifuge step are in both cases more out of the accepted range.

Table 4.4 shows the recoveries from the 'EASY' clean-up without the filter step. For AFB2 and AFG1 all values lay in the acceptable range. This is not the case for AFB1 and AFG2, where most of the recoveries exceed the accepted threshold of 110 %. The recoveries for each AFT differentiate a lot from sample to sample. These significantly high differences could show that the chosen method is not optimal. The fact that AFB1 and AFG2 recoveries don't lay in the accepted range adds to this assumption.

When comparing Table 4.3 and Table 4.4, it is clear that the recoveries without the filter become lower and fall into a more acceptable range. Adding the filter step seems promising as it improves the recoveries. However, there is no clear trend visible between the different AFTs. For AFB1 the recovery rises when the filter is left out. This is not the case for the other three AFTs. Their recoveries decline after adding a filter step.

The results in Table 4.3 and Table 4.4 show an increase in concentration (recovery > 100%) for a majority of the studied AFTs. This means that, according to the detected response, the final AFT concentration is higher than the spiked concentration before analysis. This can likely not be explained by coincidence and is probably a result of a matrix effect. Matrix effects can lead to mistakes in the quantification or identification results of the aflatoxin analysis. In this case, the effect on the quantification is visible. The influence of the matrix caused an increase in response, also called ion enhancement. (42,43)

Matrix effects are dependent on the nature of the sample. Some substances of the matrix can influence the intensity of the signal when co-eluted with the analyte. This shows that selecting the best clean-up procedure is crucial to minimise these effects. (42,43) The 'EASY' approach is not ideal to follow. The outcomes are not a representation of the real AFT concentration present in the peanuts. Due to this obtained result, the decision was

made to proceed with a matrix-matched calibration curve. This is with hopes of obtaining highly reliable data from these analyses.

5.1.4 Comparison

The best approach to follow seems the ‘dSPE’ approach without the extra centrifuge step in the end. The final decision for using this approach is based on the more accurate results that were obtained with this method. The recoveries seem to be more reliable because the influence of the matrix effect is not as present in this approach. A second reason for choosing this clean-up is that the filter step can be left out. Which saves time without influencing the results negatively. The ‘dSPE’ approach also needs less of the ground peanuts for analysing. One gram instead of five grams. The amounts of used solvents are less. Each sample gets 5 ml water and 5 ml of a formic acid/ acetonitrile mixture instead of 10 ml hexane, 10 ml water, and 15 ml acetonitrile. Which makes it more efficient and saves resources and money. Another advantage of the ‘dSPE’ is that a smaller volume has to be dried under the nitrogen flow. One milliliter instead of five. This saves some time and nitrogen. (6,27)

5.2 SCREENING USING IM-MS-TOF

5.2.1 Calibration curves

The strength of the association between two variables can be evaluated through correlation coefficient R^2 as already explained in chapter 5.1.1. In this calibration curve, these two variables are the spiked AFT concentration and the measured peak area after analysis. (40) As displayed in Table 4.5, the R^2-values calculated for the calibration curve in solvent are all higher than 0.995. This means that the spiked concentrations are strongly associated with the results of the QQQ UHPLC-MS/MS analyse, the AUC. This calibration curve can now be used for determining AFT concentrations when the AUC is measured by the QQQ UHPLC-MS/MS. This is different for the calibration curve made in matrix and

solvent, seen in Table 4.11. None of the determined R^2-values exceed the limit of 0.995. The association between the spiked AFT concentration and the AUC is lower. The use of this calibration curve can be less accurate.

Tables 4.6 until 4.15 show the found data about the masses, retention times, and the CCS values of each AFT in each concentration level using IM-MS-TOF in ESI^+ mode. The maximum allowed mass error for targeted screening using this technique is 2 ppm. For untargeted screening, this maximum level lies between 2 and 5 ppm. This mass error tells something about the accuracy of measurement. It shows how close the observed value lies to the true value. (44,45) The calculated mass error for each AFT lies far below the 2 ppm threshold, with 0.6 ppm being the biggest error.

The RT of each AFT is constant over the whole concentration range. The RT is independent of the concentration. The observed RT lays close to the expected RT. Delta RT is 0.08 min for each AFT in the solvent calibration curve and 0.09 min for each AFT in the matrix calibration curve. This could show that the RT is influenced by the matrix in which the analytes are found and analysed.

As stated in literature is the CCS database, studied in (L. Righetti et al, 2020), valid to be used in any IM-MS-TOF instrument as long as the error is not higher than ± 2 %. (36) This is in line with the results. All delta CCS values lay far below this threshold, with the highest CCS error only being 0.36 %.

CCS values are only dependent on the structure of the molecule and independent of the concentration and the matrix. (36) This is confirmed by the observed CCS values. For AFB1 this CCS value is 163.04 Å. Only for the 1 ppb spike was the CCS value 163.14 Å. This trend is seen for the other AFTs. For all of them, the observed CCS are slightly higher than for the other concentration levels. This can likely be explained by the sensitivity of the instrument. The delta CCS for all these values is still way below the instrumental error threshold and is considered acceptable. The CCS values are also independent of the complexity of the matrix. (36) This is confirmed by comparing the observed CCS in solvent with the observed CCS in matrix and solvent. (Table 4.12 until Table 4.15) For each AFT separately, the four concentration levels have the exact same observed CCS. For example,

AFB1 has an observed value of 163.1 Å for each concentration. The small difference with the observed CCS value for AFB1 in the calibration curve with only solvent can be disregarded. 163.1 Å for the matrix and solvent calibration samples opposed to 163.04 Å for the ones with only solvent.

5.2.2 Chromatograms

The chromatograms shown in Figure 4.1, Figure 4.3, Figure 4.5, and Figure 4.7 belong to respectively AFB1, AFB2, AFG1, and AFG2. Each chromatogram displays the intensity (counts) in function of the RT (min). They all have a good signal and no background noise can be seen. Each figure has one clear peak. This means that the clean-up during the sample preparation went well. No other peaks from for example the matrix are visible.

The chromatograms shown in Figure 4.2, Figure 4.4, Figure 4.6, and Figure 4.8 belong respectively to AFB1, AFB2, AFG1, and AFG2. Differently from the previously mentioned chromatograms, these present the intensity (counts) in function of the DT (ms). All of these chromatograms have two peaks. A small and a big peak. This means that each AFT has at least two different velocities of movement through the mobility chamber. The two different DTs can be interpreted as two different forms of each AFT. The big peak belongs to the protonated form $[M + H]^+$. The small peak belongs to the other formed adducts of the AFTs, namely the $[M + Na]^+$ and the $[M + K]^+$- adduct. (38,46)

5.2.3 The mobility 3D-plots

Figure 4.9 shows two yellow points with a RT of around 7 minutes, this corresponds with the RT found for AFB1 in tables 4.6 until 4.10 and tables 4.12 until 4.15. This RT is observed to be respectively 6.93 min and 6.92 min. The two different DTs can be contributed to the different forms of AFB1. The protonated form has a different drift time from the other adducts because they have a different residence time in the mobility chamber. On this graph, it is not visible how many forms of AFB1 are present. However, there is certainly at least one other form than the protonated form $[M + H]^+$ present.

Figure 4.10 confirms that there are two different DTs. However, it also shows that there are more than two forms of AFB1 present. This is proven in the graph by the three different *m/z*-values. The protonated form of AFB1 has an *m/z*-value of 313.31 Da. If a sodium ion with a mass of 22.99 Da is added this *m/z*-value would rise to 335.29 Da. If AFB1 becomes a potassium adduct the *m/z*-value would increase to a value of 351.4 Da. Figure 4.11 confirms the presence of the three forms of AFB1, shown by the three *m/z*-values. It also confirms that all three forms are indeed AFB1 because of the same RT. From these three figures, we can conclude that three forms of AFB1 are present: the protonated form $[M + H]^+$, the sodium form $[M + Na]^+$, and the potassium form $[M + K]^+$.

5.2.4 The peanuts from Piacenza, Italy

The peanuts were found to be not contaminated with AFTs. This is in line with ongoing research in the lab. Peanuts from the same fields are being analysed on the presence of mycotoxin-producing fungi. These researchers didn't find any traces of *A. flavus* or *A. parasiticus,* the two main producers of AFB1, AFB2, AFG1, and AFG2. (12) This means that finding no AFTs in the peanut samples could be accurate. The same researchers found some traces of fungi from the genus *Fusarium*. Beauvericin (BEA) is a product of *Fusarium*. (47–49) The detection of BEA is possible because IM-MS-TOF does a quick screening using an existing library (36) of known CCS values, known *m/z*-values, and known RTs. The detection of BEA and the lack of detected AFTs is consistent with the fungal profile found by other researchers in the lab. This research is still under investigation. No statements can be made about the concentrations of BEA, as the extraction was only targeted and validated for AFTs. It is not known if any of the BEA was lost during the sample preparation. So no conclusions can be made about the BEA concentrations. This investigation is still ongoing.

5.2.5 Comparison with AFT concentrations in other countries

The peanuts grown on the fields in Piacenza, Italy are not contaminated with AFTs. These results can be compared to other studies that evaluate the AFT presence in peanuts

produced in other countries. A study on multiple peanut samples taken from farms in Zambia shows the contamination of these nuts with AFTs. The total AFT concentration that was found ranged from 4 to 100 µg/kg. (30) In Western Kenya the same problem is seen. Between 1.45 % and 9.00 % of the observed samples contained AFT levels between 4 µg/kg and 20 µg/kg. 2.70 to 10 % of the peanut samples even exceeded the threshold of 20 µg/kg. (50) These concentrations are a lot higher than 4 µg/kg, the tolerated AFT levels set by the EU. (21) The results found in this thesis are promising for the production of peanuts in Italy as they seem to be safer than peanuts grown in some other countries. The application of GAP can lead to lower aflatoxin contaminations. (51) This could be an explanation for this difference in AFT occurrence. Farmers in Italy are more likely to apply better GAP than countries in some parts of Africa. The average Italian farmer has more access to knowledge about avoiding mycotoxin contamination of the growing crops. They generally also have more resources to be able to apply GAP. The fact that Italian climate is less optimal for aflatoxigenic fungi growth could be another contributing factor. (11,51)

6. CONCLUSION

The best approach to follow seemed the ‘dSPE’ approach without the extra centrifuge step. The final decision for using this approach was based on the better recoveries that were obtained using this approach. The recoveries seemed to be more reliable because the influence of the matrix effect is not as present as in the ‘EASY’ approach. A second reason for choosing this clean-up is that the filter step could be left out. Which saves time without influencing the results negatively. Lastly, this method needed less ground peanuts, solvents, and nitrogen. Making this method cheaper and faster to perform. The method validation was done using triple QQQ UHPLC-MS/MS. And the optimised method is ready for analysing other peanuts in the future.

The peanuts of interest are the peanuts grown in Piacenza, Italy. After screening with IM-MS-TOF, they were found to be not contaminated with AFTs. No peaks were visible in the chromatograms. This is in line with ongoing research in the lab. In this research, no traces of *A. flavus* or *A. parasiticus* were found. These fungi are the two main producers of AFB1, AFB2, AFG1, and AFG2. On the other hand, some traces of fungi from the genus *Fusarium* were discovered. Beauvericin (BEA) is a product of *Fusarium.* Some traces of BEA were present in the peanuts, according to the screening. When these results are compared to other countries such as Kenya or Zambia, these Italian peanuts seem a lot safer. This is promising for the future of the peanut production in Italy. The better results of the Italian peanuts can be due to the better application of GAP. Another factor is the less optimal climate in Italy for aflatoxigenic fungal growth in peanuts.

7. BIBLIOGRAPHY

1. Rushing BR, Selim MI. Aflatoxin B1: A review on metabolism, toxicity, occurrence in food, occupational exposure, and detoxification methods. Vol. 124, Food and Chemical Toxicology. Elsevier Ltd; 2019. p. 81–100.
2. Kumar P, Mahato DK, Kamle M, Mohanta TK, Kang SG. Aflatoxins: A global concern for food safety, human health and their management. Vol. 7, Frontiers in Microbiology. Frontiers Media S.A.; 2017.
3. Varga E, Glauner T, Berthiller F, Krska R, Schuhmacher R, Sulyok M. Development and validation of a (semi-)quantitative UHPLC-MS/MS method for the determination of 191 mycotoxins and other fungal metabolites in almonds, hazelnuts, peanuts and pistachios. Anal Bioanal Chem. 2013 Jun;405(15):5087–104.
4. Alshannaq A, Yu JH. Occurrence, toxicity, and analysis of major mycotoxins in food. Vol. 14, International Journal of Environmental Research and Public Health. MDPI; 2017.
5. Mahato DK, Lee KE, Kamle M, Devi S, Dewangan KN, Kumar P, et al. Aflatoxins in Food and Feed: An Overview on Prevalence, Detection and Control Strategies. Vol. 10, Frontiers in Microbiology. Frontiers Media S.A.; 2019.
6. Alsharif AMA, Choo YM, Tan GH. Detection of five mycotoxins in different food matrices in the malaysian market by using validated liquid chromatography electrospray ionization triple quadrupole mass spectrometry. Toxins (Basel). 2019 Apr 1;11(4).
7. Dhanasekaran D, Shanmugapriya S, Thajuddin N, Panneerselvam A. Aflatoxins and Aflatoxicosis in Human and Animals. In: Aflatoxins - Biochemistry and Molecular Biology. InTech; 2011.
8. Zhang K, Banerjee K. A Review: Sample Preparation and Chromatographic Technologies for Detection of Aflatoxins in Foods. Vol. 12, Toxins. MDPI AG; 2020.
9. Alshannaq A, Yu JH. Analysis of E.U. Rapid Alert System (RASFF) Notifications for Aflatoxins in Exported U.S. Food and Feed Products for 2010–2019. Toxins (Basel). 2021 Feb 1;13(2).
10. Meneely JP, Kolawole O, Haughey SA, Miller SJ, Krska R, Elliott CT. The Challenge of Global Aflatoxins Legislation with a Focus on Peanuts and Peanut Products: A Systematic Review. Exposure and Health. Springer Science and Business Media B.V.; 2022.
11. Payne GA. Mycotoxins and Product Safety. In: Peanuts: Genetics, Processing, and Utilization. Elsevier Inc.; 2016. p. 347–61.
12. Schrenk D, Bignami M, Bodin L, Chipman JK, del Mazo J, Grasl-Kraupp B, et al. Risk assessment of aflatoxins in food. EFSA Journal. 2020 Mar 1;18(3).
13. Pitt JI, Hocking AD. Mycotoxins in Australia: Biocontrol of aflatoxin in peanuts. Vol. 162, Mycopathologia. 2006. p. 233–43.
14. Bernáldez V, Córdoba JJ, Magan N, Peromingo B, Rodríguez A. The influence of ecophysiological factors on growth, aflR gene expression and aflatoxin B1 production by a type strain of Aspergillus flavus. LWT. 2017 Sep 15;83:283–91.
15. Yabe K, Nakajima H. Enzyme reactions and genes in aflatoxin biosynthesis. Vol. 64, Applied Microbiology and Biotechnology. 2004. p. 745–55.
16. De Baere S, Ochieng PE, Kemboi DC, Scippo ML, Okoth S, Lindahl JF, et al. Development of High-Throughput Sample Preparation Procedures for the Quantitative Determination of Aflatoxins in Biological Matrices of Chickens and Cattle Using UHPLC-MS/MS. Toxins (Basel). 2023 Jan 1;15(1).
17. IARC (International Agency for Research on Cancer. Aflatoxins. IARC Monographs, 82. 2002. p. 171–300.
18. Wang H, Zhou XJ, Liu YQ, Yang HM, Guo QL. Determination of aflatoxin M1 in milk by triple quadrupole liquid chromatography-tandem mass spectrometry. Food Additives and Contaminants - Part A. 2010;27(9):1261–5.

19. Chemicals and Materials What is a LD 50 and LC 50 ? 2018 Nov.
20. Jaimez J, Fente CA, Vazquez BI, Franco CM, Cepeda A, Mahuzier G, et al. Application of the assay of aflatoxins by liquid chromatography with fluorescence detection in food analysis [Internet]. Vol. 882, Journal of Chromatography A. 2000. Available from: www.elsevier.com/locate/chroma
21. Dorner JW. Management and prevention of mycotoxins in peanuts. Food Addit Contam Part A Chem Anal Control Expo Risk Assess. 2008;25(2):203–8.
22. Van Egmond HP. WORLDWIDE REGULATIONS FOR MYCOTOXINS. 2002.
23. Mupunga I, Mngqawa P, Katerere DR. Peanuts, aflatoxins and undernutrition in children in Sub-Saharan Africa. Vol. 9, Nutrients. MDPI AG; 2017.
24. Smith LE, Stoltzfus RJ, Prendergast A. Food chain mycotoxin exposure, gut health, and impaired growth: A conceptual framework. Vol. 3, Advances in Nutrition. 2012. p. 526–31.
25. P C Turner, A Sylla, Y Y Gong, M S Diallo, A E Sutcliffe, A J Hall, et al. Reduction in exposure to carcinogenic aflatoxins by postharvest intervention measures in west Africa [Internet]. 2005. Available from: www.thelancet.com
26. Xie L, Chen M, Ying Y. Development of Methods for Determination of Aflatoxins. Vol. 56, Critical Reviews in Food Science and Nutrition. Taylor and Francis Inc.; 2016. p. 2642–64.
27. Sartori AV, De Mattos JS, Souza YP, Dos Santos RP, Paulino de Moraes MH, Da Nóbrega AW. Determination of aflatoxins M1, M2, B1, B2, G1 and G2 in peanut by modified QuEChERS method and ultra-high performance liquid chromatography-tandem mass spectrometry. Vigilância Sanitária em Debate. 2014 Nov 27;0(0).
28. Arya SS, Salve AR, Chauhan S. Peanuts as functional food: a review. Vol. 53, Journal of Food Science and Technology. Springer India; 2016. p. 31–41.
29. Settaluri VS, Kandala CVK, Puppala N, Sundaram J. Peanuts and Their Nutritional Aspects—A Review. Food Nutr Sci. 2012;03(12):1644–50.
30. Njoroge SMC. A critical review of aflatoxin contamination of peanuts in Malawi and Zambia: The past, present, and future. Vol. 102, Plant Disease. American Phytopathological Society; 2018. p. 2394–406.
31. Kamika I, Mngqawa P, Rheeder JP, Teffo SL, Katerere DR. Mycological and aflatoxin contamination of peanuts sold at markets in Kinshasa, Democratic Republic of Congo, and Pretoria, South Africa. Food Addit Contam Part B Surveill. 2014;7(2):120–6.
32. Bennett JW, Klich M. Mycotoxins. Vol. 16, Clinical Microbiology Reviews. 2003. p. 497–516.
33. Mahfuz M, Gazi MA, Hossain M, Islam MR, Fahim SM, Ahmed T. General and advanced methods for the detection and measurement of aflatoxins and aflatoxin metabolites: a review. Vol. 39, Toxin Reviews. Taylor and Francis Ltd; 2020. p. 123–37.
34. Morris CB, Poland JC, May JC, McLean JA. Fundamentals of Ion Mobility-Mass Spectrometry for the Analysis of Biomolecules. In: Methods in Molecular Biology. Humana Press Inc.; 2020. p. 1–31.
35. Righetti L, Bergmann A, Galaverna G, Rolfsson O, Paglia G, Dall'Asta C. Ion mobility-derived collision cross section database: Application to mycotoxin analysis. Anal Chim Acta. 2018 Jul 19;1014:50–7.
36. Righetti L, Dreolin N, Celma A, McCullagh M, Barknowitz G, Sancho J V., et al. Travelling wave ion mobility-derived collision cross section for mycotoxins: Investigating interlaboratory and interplatform reproducibility. J Agric Food Chem. 2020 Sep 30;68(39):10937–43.
37. Gabelica V, Shvartsburg AA, Afonso C, Barran P, Benesch JLP, Bleiholder C, et al. Recommendations for reporting ion mobility Mass Spectrometry measurements. Vol. 38, Mass Spectrometry Reviews. John Wiley and Sons Inc.; 2019. p. 291–320.
38. Yogendrarajah P, Van Poucke C, De Meulenaer B, De Saeger S. Development and validation of a QuEChERS based liquid chromatography tandem mass spectrometry method for the determination of multiple mycotoxins in spices. J Chromatogr A. 2013 Jul 5;1297:1–11.

39. Augustin Mihalache O, Carbonell-Rozas L, Cutroneo S, Dall'Asta C. Multi-mycotoxin determination in plant-based meat alternatives and exposure assessment. Food Research International. 2023 Jun 1;168.
40. Camirand Lemyre F, Chalifoux K, Desharnais B, Mireault P. Squaring Things Up with R2: What It Is and What It Can (and Cannot) Tell You. J Anal Toxicol. 2022 May 1;46(4):443–8.
41. Ouakhssase A, Chahid A, Choubbane H, Aitmazirt A, Addi EA. Optimization and validation of a liquid chromatography/tandem mass spectrometry (LC-MS/MS)method for the determination of aflatoxins in maize. Heliyon. 2019 May 1;5(5).
42. Zhou W, Yang S, Wang PG. Matrix effects and application of matrix effect factor. Vol. 9, Bioanalysis. Future Medicine Ltd.; 2017. p. 1839–44.
43. Trufelli H, Palma P, Famiglini G, Cappiello A. An overview of matrix effects in liquid chromatography-mass spectrometry. Vol. 30, Mass Spectrometry Reviews. 2011. p. 491–509.
44. Time of Flight The Power of Accurate Mass.
45. Brenton AG, Godfrey AR. Accurate mass measurement: Terminology and treatment of data. J Am Soc Mass Spectrom. 2010 Nov;21(11):1821–35.
46. Ventura M, Gómez A, Anaya I, Díaz J, Broto F, Agut M, et al. Determination of aflatoxins B1, G1, B2 and G2 in medicinal herbs by liquid chromatography-tandem mass spectrometry. J Chromatogr A. 2004 Sep 3;1048(1):25–9.
47. Moretti A, Susca A. Mycotoxigenic Fungi Methods and Protocols [Internet]. 2017. Available from: http://www.springer.com/series/7651
48. Ekwomadu TI, Akinola SA, Mwanza M. Fusarium mycotoxins, their metabolites (Free, emerging, and masked), food safety concerns, and health impacts. Int J Environ Res Public Health. 2021 Nov 1;18(22).
49. Caloni F, Fossati P, Anadón A, Bertero A. Beauvericin: The beauty and the beast. Vol. 75, Environmental Toxicology and Pharmacology. Elsevier B.V.; 2020.
50. Mutegi CK, Ngugi HK, Hendriks SL, Jones RB. Prevalence and factors associated with aflatoxin contamination of peanuts from Western Kenya. Int J Food Microbiol. 2009 Mar 15;130(1):27–34.
51. Code of practice for the prevention and reduction of mycotoxin contamination in cereals. 2003.

Master dissertation submitted to the faculty of Pharmaceutical Sciences, performed in collaboration with the University of Parma.

Promotor: Prof. dr. Marthe De Boevre
Second promotor: Prof. dr. Chiara Dall'Asta

Commissioners: Dr. Alfonso Narvaez and Dr. Tullia Tedeschi

This master dissertation is an examination document that not necessarily has been corrected for eventual mistakes. The information, conclusions, and points of view in this master dissertation are those of the author and do not necessarily represent the opinion of the promoter or his/her research group.